can play a pivotal role in the regulation of vascular tonus.[7–10] Moreover, WNK signaling is positively controlled by aldosterone, angiotensin II, and insulin, which may contribute to hypertension in patients with hyperaldosteronism and hyperinsulinemia.[11–15] Therefore, drugs that inhibit this signal cascade are expected to treat hypertension through dual actions (*i.e.*, NaCl diuresis and vasodilation), and may be particularly effective in patients with hyperaldosteronism or hyperinsulinemia. In this study, we focused on the SPAK kinase because SPAK knockout mice were not fatal and displayed hypotension with low NCC and NKCC1 phosphorylation in mouse kidney and aorta, respectively.[16,17] The purposes of this study were to develop a new high-throughput screening system using ELISA and to discover novel SPAK inhibitors from libraries of small-molecule compounds and existing drugs.

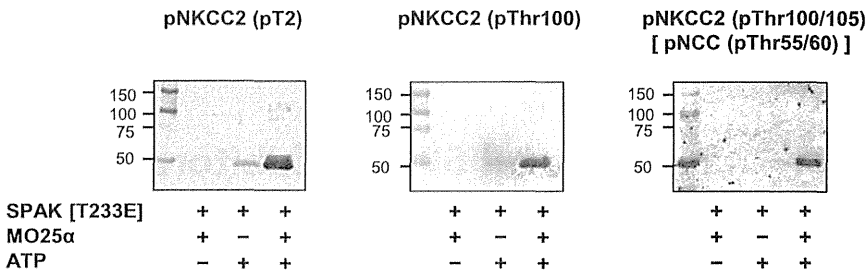


**Figure 1.** Confirmation of the *in vitro* phosphorylation reaction of GST-NKCC2 using three different anti-phospho-NKCC2 antibodies. GST-NKCC2 is incubated with GST-SPAK [T233E] in the absence or presence of MO25α. Subsequently, the GST-NKCC2 phosphorylation reaction is confirmed by the immunoblotting by using three different anti-phospho-NKCC2 antibodies: anti-pNKCC2 (pT2), pNKCC2 (pThr100), and pNKCC2 (pThr100/105)[pNCC (pThr50/55)]. The most dramatic increase in ATP-dependent NKCC2 phosphorylation is observed in the presence of GST-MO25α.

## RESULTS

### Development of an ELISA System for the Detection of SPAK-Regulated NKCC2 Phosphorylation

To find novel inhibitors of the SPAK kinase, we developed a new screening system using ELISA. Previous studies have shown that SPAK possessed very low kinase activity *in vitro*, which hampered a high-throughput screening of the inhibitors.[18] In this study, we adopted a combination strategy that included the recombinant SPAK [T233E] protein, in which the T-loop Thr residue phosphorylated by WNK isoforms was mutated to Glu to mimic phosphorylation, and the Mouse protein 25α (MO25α) to detect the SPAK-regulated phosphorylation more sensitively.[18–20] MO25α is an enhancer of SPAK kinase. We used a fragment of human NKCC2 (residues 1–174) including SPAK phosphorylation sites as a substrate for SPAK because NKCC2 phosphorylation has been known to be the most detectable during *in vitro* experiments.[18] They were all prepared as glutathione *S*-transferase (GST) fusion proteins and purified.

First, to determine whether the kinase reaction functions properly *in vitro*, the GST-NKCC2 phosphorylation reaction was confirmed by the immunoblotting of three different anti-phospho-NKCC2 antibodies. As shown in Figure 1, the most dramatic increase in ATP-dependent NKCC2 phosphorylation was observed in the presence of GST-MO25α. Next, we tested the utility of these anti-phospho-NKCC2 antibodies in the ELISA system. First, the ELISA plates were coated with 5 pmol of GST-NKCC2 [1–174] per well. After this, the kinase reaction was induced on the ELISA plate using GST-SPAK [T233E] with GST-MO25α in the presence of ATP. Finally, the phosphorylation of GST-NKCC2 was detected with each anti-phospho-NKCC2 antibody. As shown in Figure 2, two of the three anti-phospho-NKCC2 antibodies, pT2 and pNKCC2 (pThr100/105), succeeded in detecting NKCC2 phosphorylation. Finally, we adopted the anti-phospho-NKCC2 (pThr100/105) antibody as a primary antibody. To determine the dose-dependent kinetics, we incubated 0.5 pmol of GST-SPAK [T233E] in the presence of different concentrations of substrate, GST-NKCC2, and ATP. *In vitro* GST-NKCC2 phosphorylation increased according to the amount of coated GST-NKCC2 (Supplemental Figure 1A) and ATP concentrations (Supplemental Figure 1B). On the basis of these results, we determined that the optimum amounts of GST-NKCC2 and ATP were 5 pmol/well and 0.1 mM, respectively, in this screening.

### ELISA Screening of a Small-Molecule Compound Library for SPAK Inhibitors

We applied this newly developed indirect ELISA system for screening approximately 20,000 small-molecule compounds

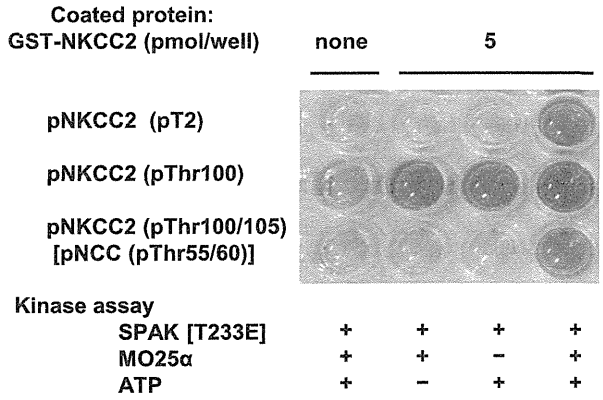


**Figure 2.** Kinase assay and detection of phosphorylated NKCC2 in the ELISA system. GST-NKCC2 [1–174] is coated to each well of the ELISA plate and incubated with GST-SPAK [T233E] in the presence of GST-MO25α. Anti-p-NKCC2 (pT2) and p-NKCC2 (pThr100/105) [p-NCC (pTh50/55)] antibodies succeed in detecting NKCC2 phosphorylation. Anti-p-NKCC2 (pThr100) antibody is not appropriate for ELISA, because a nonspecific blue color change also develops in negative control wells.

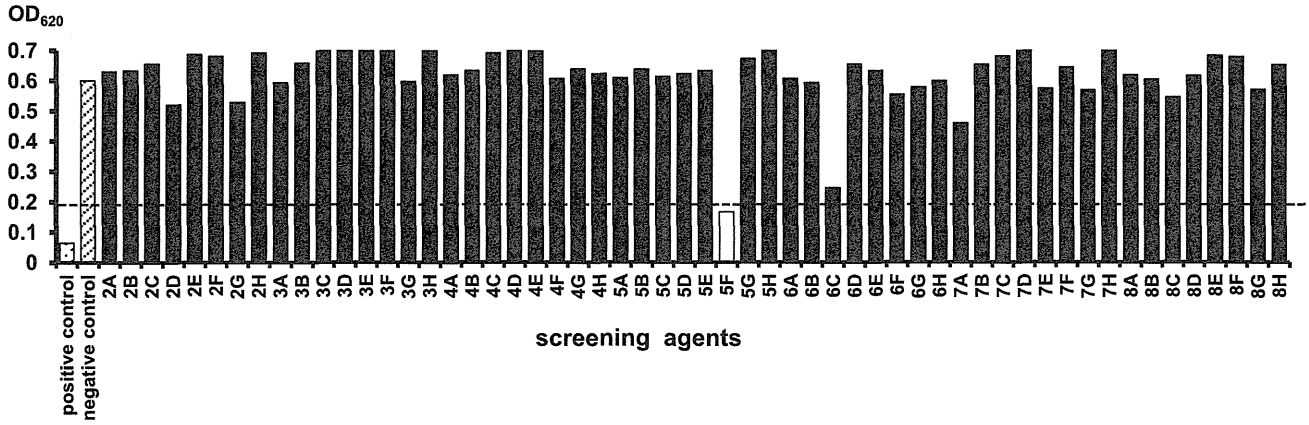


**Figure 3.** Representative figure of primary screening of SPAK inhibitors in the newly developed ELISA system. Each compound is added in the kinase reaction at a final concentration of 50 $\mu$M. As a positive control indicating nonphosphorylation of NKCC2, ATP-free kinase buffer is used. A kinase reaction without any compounds is used as a negative control for screening. The arbitrary cut-off value of $OD_{620}$ is set to 0.2. The compound shown as a white bar is regarded as a positive compound having a strong inhibitory effect on SPAK-regulated NKCC2 phosphorylation.

owned by the Tokyo Medical and Dental University Chemical Biology Screening Center. We actually performed the screening by adding each compound at 50 $\mu$M into the kinase reaction buffer and obtained the signals at 620 nm. Representative results of the initial screening are shown in Figure 3. As a result of the initial screening of 21,727 compounds, we found 757 positive compounds. In the secondary assay of these positive compounds, the inhibitory effects were almost the same as those observed in the primary assay (reproducibility was >80%), indicating that our system was solid (Supplemental Figure 2). Subsequently, we carefully narrowed down the candidates by gradually decreasing the final concentrations of the compounds (50–10 $\mu$M, data not shown). Finally, we discovered Stock 1S-14279 (1S-14279; PubChem CID 01676700) that showed the highest SPAK inhibitory effect. Figure 4A shows the chemical structure of 1S-14279. The median inhibitory concentration ($IC_{50}$) value of 1S-14279 for SPAK was 0.26 $\mu$M (Figure 4B).

## Surface Plasmon Resonance Analyses of the Binding Interactions between 1S-14279 and SPAK Kinase

With our ELISA screening system, it was unclear whether 1S-14279 directly interacts with SPAK. To determine the interaction of 1S-14279 and SPAK, we performed a binding assay using the Biacore system. Gradient concentrations (1.6–12.5 $\mu$M) of 1S-14279 were injected into GST-SPAK–immobilized flow cells. As shown in Figure 4C, 1S-14279 directly bound to SPAK in a concentration-dependent manner. When a simple 1:1 binding model was fitted, the equilibrium constant KD was 7.0E-6 (M).

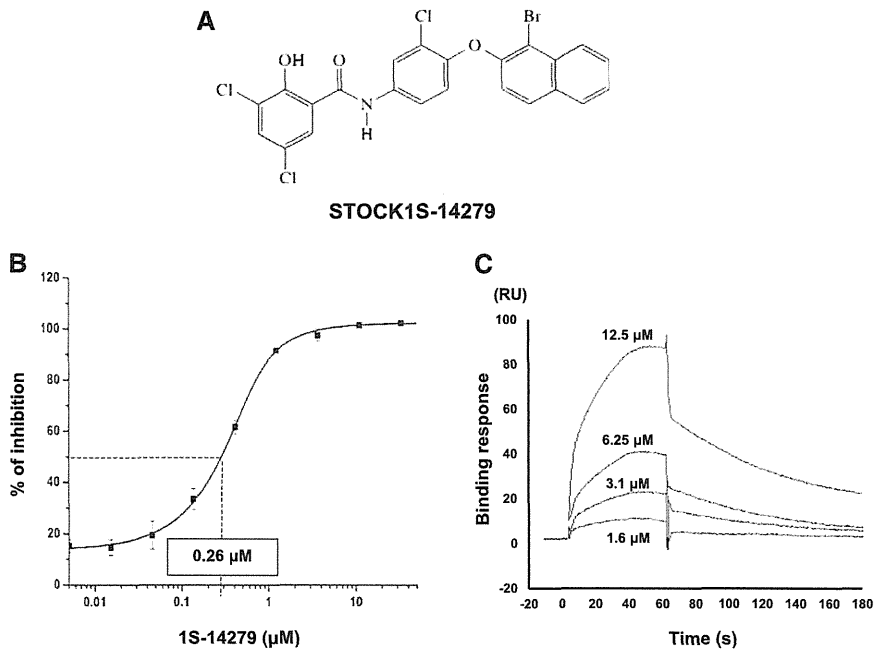


**Figure 4.** A hit compound obtained from the small-molecule compound library. (A) Chemical structure and substance name of a hit compound. (B) Confirmation of the inhibitory effect of 1S-14279 in the ELISA system. 1S-14279 is added at various concentrations (0.005–50 $\mu$M). The $IC_{50}$ value of 1S-14279 is 0.26 $\mu$M ($n$=3, mean±SEM). (C) Surface plasmon resonance analysis of 1S-14279 binding to SPAK [T233E]. 1S-14279 is applied at the indicated concentrations. Nonspecific binding to the reference cell is subtracted from each sensorgram to obtain the specific-binding responses. 1S-14279 interacts with SPAK in a concentration-dependent manner. RU, resonance unit.

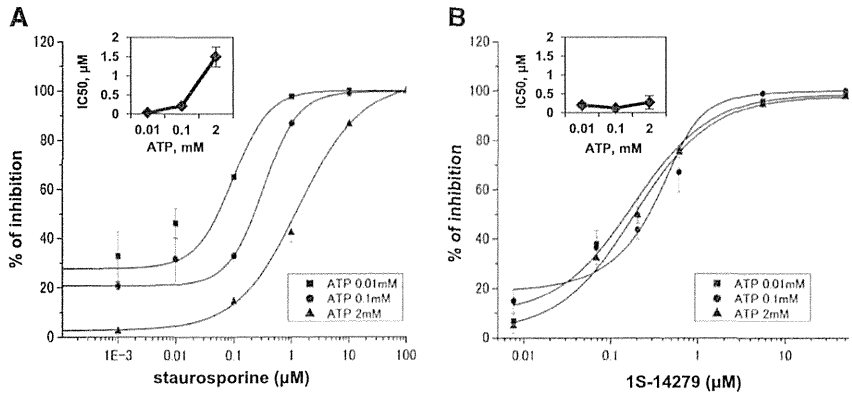


**Figure 5.** Effect of increasing concentrations of staurosporine and 1S-14279 on SPAK activity at different ATP concentrations in the ELISA system. (A and B) Kinetic data determined for staurosporine (A) and 1S-14279 (B). ATP concentrations in the reaction mixture vary from 0.01 to 2 mM. 1S-14279 and staurosporine are added at various concentrations (from 0.01 to 50 and from 1E-4 to 100 $\mu$M, respectively). Data points are the average of three determinations, and the error bars are ±SEM. The inner panels show $IC_{50}$ values, determined for each ATP concentrations. $IC_{50}$ results are 0.05, 0.27, and 1.6 $\mu$M for staurosporine at 0.01, 0.1, and 2 mM ATP, respectively. $IC_{50}$ values of 1S-14279 are not affected by ATP concentration (0.21, 0.13, and 0.26 $\mu$M at 0.01, 0.1, and 2 mM ATP, respectively).

### Inhibitory Effect of 1S-14279 on SPAK Activity Was Independent of ATP Concentrations

Next, we clarified whether the kinase inhibitory effect of 1S-14279 was due to the competition for ATP bound to SPAK because many kinase inhibitors were ATP competitive. To clarify this issue, we tested the inhibitory effect of 1S-14279 and staurosporine (a nonspecific kinase inhibitor) at different ATP concentrations. Staurosporine interacts with up to 253 human protein kinases with high affinity and inhibits SPAK activity.[21,22] As shown in Figure 5A, the $IC_{50}$ values of staurosporine as an ATP-competitive inhibitor varied 30-fold (0.05 $\mu$M and 1.5 $\mu$M at 0.01 mM and 2 mM ATP, respectively). By contrast, the $IC_{50}$ values of 1S-14279 did not alter with the ATP concentration tested (0.21 $\mu$M and 0.26 $\mu$M at 0.01 mM and 2 mM ATP, respectively) (Figure 5B). These

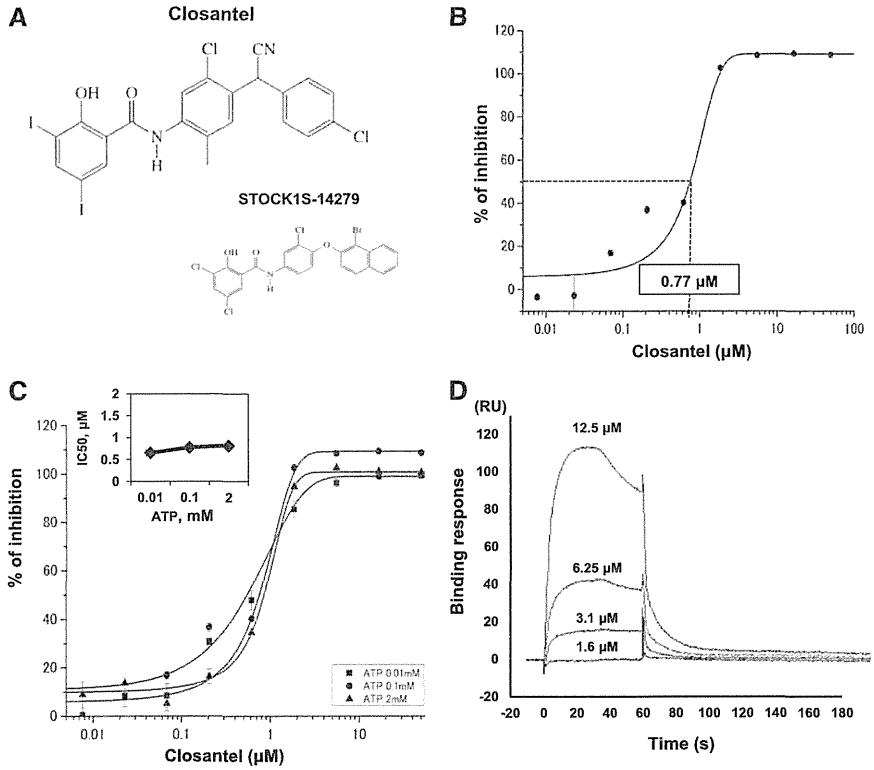


**Figure 6.** A hit compound obtained from a library of existing drugs. (A) Chemical structure of Closantel and its comparison with 1S-14279. (B) Confirmation of inhibitory effects of Closantel in the ELISA system. The compound is added at various concentrations (0.005–100 $\mu$M). The $IC_{50}$ value of Closantel is 0.77 $\mu$M ($n$=3, mean±SEM). (C) Inhibitory effect of increasing concentrations of Closantel on SPAK activity at different ATP concentrations. Closantel is added at various concentrations (0.01–50 $\mu$M). Data points are the average of three determinations, and error bars are ±SEM. The inner panel shows $IC_{50}$ values determined for each ATP concentrations. $IC_{50}$ values for Closantel are not affected by ATP concentration (0.65, 0.77, and 0.81 $\mu$M at 0.01, 0.1, and 2 mM ATP, respectively). (D) Surface plasmon resonance analysis of Closantel binding to SPAK [T233E]. Closantel is applied at the indicated concentrations. Nonspecific binding to the reference cell is subtracted from each sensorgram to obtain the specific-binding responses. Closantel interacts with SPAK in a concentration-dependent manner. RU, resonance unit.

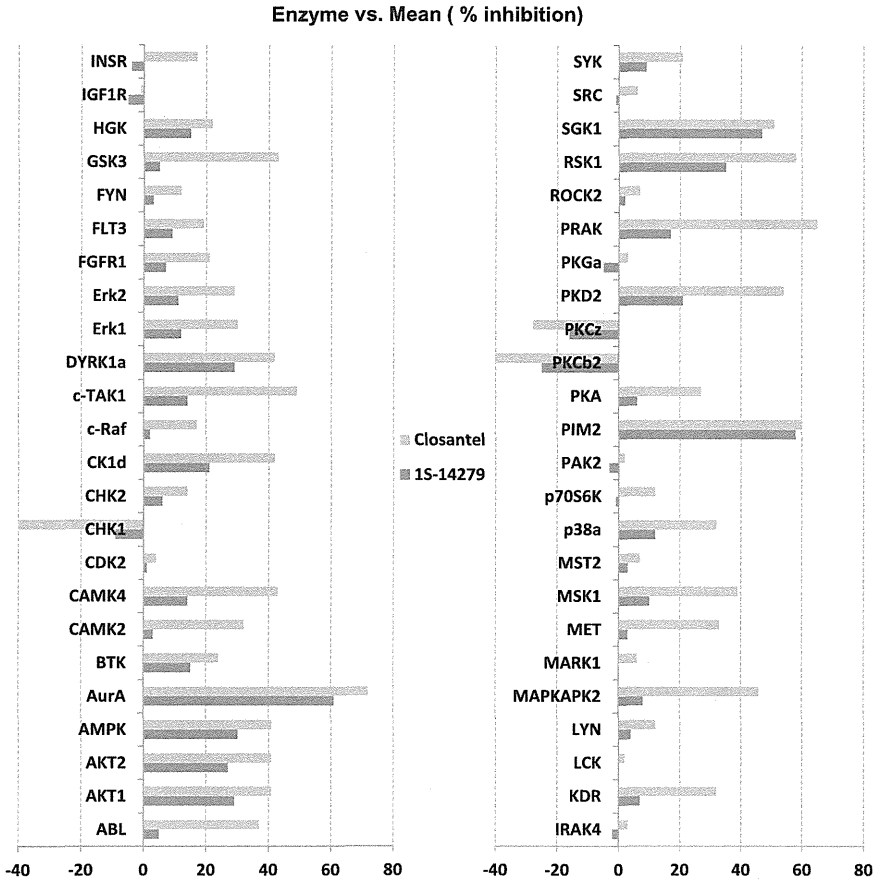


**Figure 7.** RapidKinaseTM48 panel test of 1S-14279 and Closantel. The percent inhibition of kinase activity is tested at 1.0E-05 M. Mean percent inhibition data are an average of duplicate measurements. AurA, Aurora A kinase; PIM2, Proviral Integrations of Moloney virus 2 kinase.

results clearly suggested that 1S-14279 acts as a non-ATP–competitive inhibitor for SPAK because the inhibitory effect was independent of ATP concentration.[23]

### Drug Repositioning Strategy to Identify Existing Drugs That Inhibit SPAK Kinase Activity

We further screened a library of 840 existing drugs prepared by our coauthors at Keio University to more efficiently identify clinically applicable SPAK inhibitors. We found that Closantel (*N*-[5-chloor-4-[(4-chloorfenyl)-cyanomethyl]-2-methylfenyl]-2-hydroxy-3,5-di-joodbenzamide), an anthelmintic drug, efficiently inhibited SPAK-regulated NKCC2 phosphorylation *in vitro*. Figure 6A shows the chemical structure of Closantel, which is similar in structure to 1S-14279. Figure 6B shows the results of the concentration-dependent inhibitory effect of Closantel on ELISA. The $IC_{50}$ value of Closantel was 0.77 $\mu$M. Furthermore, we tested the inhibitory effect of Closantel with different ATP concentrations. There was little change in the $IC_{50}$ values (0.65 $\mu$M and 0.81 $\mu$M at 0.01 mM and 2 mM ATP, respectively, Figure 6C); this behavior was also similar to that of 1S-14279. In the Biacore systems, Closantel directly bound to SPAK and showed relatively faster binding and dissociation than 1S-14279.

### SPAK Specificity of 1S-14279 and Closantel

To investigate the specificity of these compounds as kinase inhibitors, we conducted a profiling study in the RapidKinase48 panel. The compounds were tested at a final concentration of 1.0E-5 (M), and the kinase profiling revealed that they worked on a few serine/threonine kinases such as Aurora A kinase and Proviral Integration of Moloney virus 2 kinase, although the inhibition did not exceed 80% (Figure 7). Although SPAK kinase was not included in this panel, our ELISA assay showed an $IC_{50}$ of Closantel and 1S-14279 for SPAK in the range of 1.0E-7 (M), suggesting that both compounds have a potential to behave as specific SPAK inhibitors at lower concentrations.

### 1S-14279 and Closantel Showed Inhibitory Effects on Hypotonicity-Induced WNK-SPAK-NCC/NKCC Signaling in Mouse Renal Distal Tubule-Derived Cells and Vascular Smooth Muscle Cells

To test whether these compounds possess an *in vivo* inhibitory effect against SPAK, we used mouse renal distal tubule–derived (mpkDCT) cells and mouse vascular smooth muscle (MOVAS) cells, which endogenously express NCC and NKCC1, and performed cell-based inhibitory assays.[6,24] We used 30-minute hypotonic shock (170 mOsm/g $H_2O$) to activate WNK-SPAK-NCC/NKCC signaling.[25] Both 1S-14279 and Closantel demonstrated a dose-dependent inhibitory effect of phosphorylation of endogenous NCC (pThr53) in mpkDCT cells (Figures 8A and 9A) and of NKCC1 (pThr206) in MOVAS cells (Figures 8B and 9B). To exclude the possibility that the decrease in phosphorylation was due to nonspecific effects, we evaluated the effect of these compounds on phospho-p38 MAPK expression, which is an isolated phosphorylation event from WNK-SPAK signaling.[26] As shown in Figures 8 and 9, even with the high concentration of these compounds, the phosphorylation of p38 expression was not reduced but was slightly increased. These data support the specificity of the inhibitory effect of 1S-14279 and Closantel on SPAK activity.

### Acute Effects of 1S-14279 and Closantel in Mice

To define whether these compounds are effective in animals, we examined NCC and NKCC2 phosphorylation in the kidney and NKCC1 phosphorylation in the aorta of mice intraperitoneally

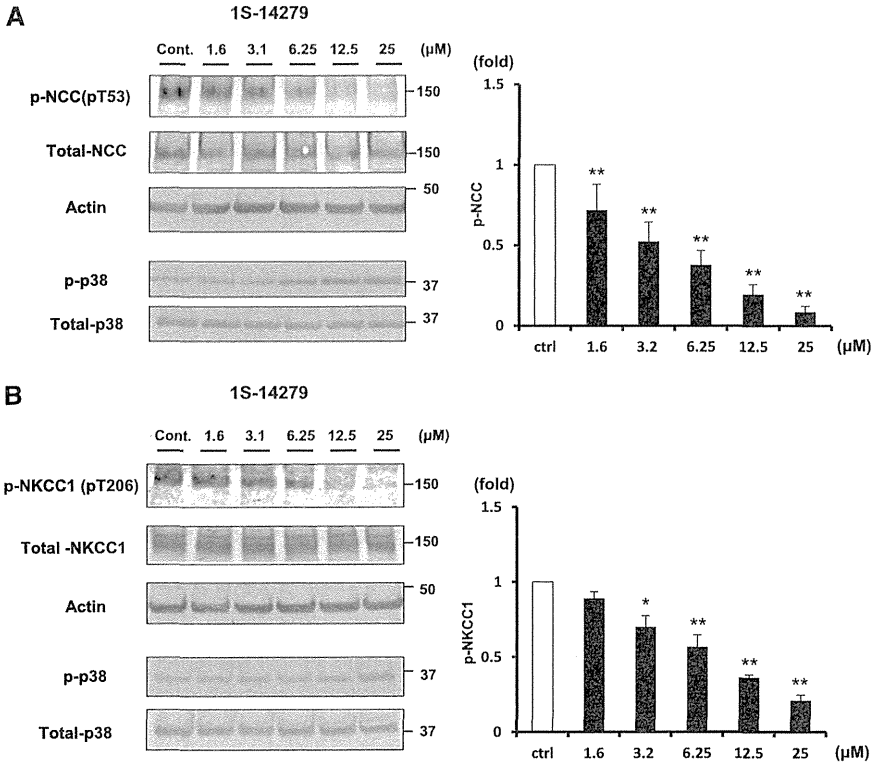


**Figure 8.** Inhibitory effect of 1S-14279 on WNK-SPAK-NCC/NKCC1 signaling in mpkDCT and MOVAS cells. (A) The left panel shows the inhibitory effect of 1S-14279 in mpkDCT cells. The phosphorylation of NCC in mpkDCT cells is drastically and dose-dependently reduced by 1S-14279 (1.6–25 $\mu$M). The right panel shows quantification of the results of the blots ($n$=4, mean±SEM). (B) The left panel shows the inhibitory effect of 1S-14279 in MOVAS cells. The phosphorylation of NKCC1 is drastically and dose-dependently reduced by 1S-14279 (1.6–25 $\mu$M). The right panel shows quantification of the results of the blots ($n$=4, mean±SEM). *$P$<0.05; **$P$<0.01. Cont/ctrl, control.

injected with 20 mg/kg of 1S-14279 or Closantel. As shown in Figures 10A and 11A, markedly reduced NCC phosphorylation (pSer71) with total NCC reduction was observed in the kidneys after 30 minutes of drug administration. On the other hand, NKCC2 phosphorylation (pThr96), which was mainly regulated by OSR1 but not SPAK,[27] was not affected. To exclude the non-specific effects of the compounds, we also evaluated the effect of these compounds on phospho-p38 MAPK expression, as mentioned in the cell-based inhibitory assay. Even with the administration of these compounds, the expression of phospho-p38 was not reduced and was slightly increased, similar to that observed in the cell-based study. Similarly, NKCC1 phosphorylation (pThr206) at the SPAK phosphorylation site was reduced in the aorta. We also followed the time course of the inhibitory effect after a single injection of 1S-14279 and Closantel. After 30 minutes of injection, the level of phosphorylated NCC rapidly decreased; however, it entirely recovered after 120 minutes (Supplemental Figure 3). The SPAK inhibitory effects of 1S-14279 and Closantel were short acting and reversible. We then chose Closantel for BP measurement because preliminary experiments revealed that mice typically died after repeated injection of 1S-14279, and Closantel showed no lethal effects. As shown in Figure 12, the acute injection of Closantel induced marked hypotension from baseline, which was greatest immediately after injection. The heart rate also decreased just after the hypotensive reaction and recovered earlier than the BP.

### Effect of Chronic Closantel Treatment in Mice

Next, we examined the effect of chronic treatment with oral Closantel. C57BL/6 mice were fed the mouse chow containing Closantel at a dosage of 300 mg/kg per day. Mice appeared to be healthy during the Closantel treatment. As shown in Figure 13, by day 7 of treatment, NCC and NKCC2 phosphorylation were markedly decreased in the kidneys, and NKCC1 phosphorylation was reduced in the aorta. However, BP was not decreased by Closantel, and we observed no significant differences in serum and urine electrolytes between the Closantel and control groups (Supplemental Figure 4, Supplemental Table 1).

## DISCUSSION

We previously reported that the constitutive activation of the WNK-OSR1/SPAK-NCC signal cascade is the major pathogenic mechanism of PHAII.[28–30] The increased level of NCC phosphorylation induces excessive NaCl reabsorption and causes salt-sensitive hypertension. WNK-OSR1/SPAK kinase also phosphorylates and activates NKCC1 in vascular smooth muscle cells and leads to vasoconstriction.[7–10] Furthermore, we revealed that this cascade was activated not only in PHAII but also in hyperinsulinemic conditions and could also cause salt-sensitive hypertension.[13] Therefore, drugs that inhibit this signal cascade could become new antihypertensive drugs that have dual effects as a diuretic and vasodilator and could be particularly beneficial for patients with hyperinsulinemia (*e.g.*, metabolic syndrome and obesity). However, directly inhibiting WNK kinases could have a risk of unexpected adverse reactions because homozygous WNK1 and OSR1 knockout mice are embryonically lethal. On the other hand, it was previously reported that SPAK knockout mice were not fatal and displayed hypotension with low NCC and NKCC1 phosphorylation in the kidney and aorta, respectively.[16,17] Thus, the SPAK kinase may become a prime target for drug development with the inhibition this signal cascade.

In this study, we sought to develop a new screening system using ELISA that could demonstrate SPAK-regulated phosphorylation *in vitro*. As a result of our screening, we discovered

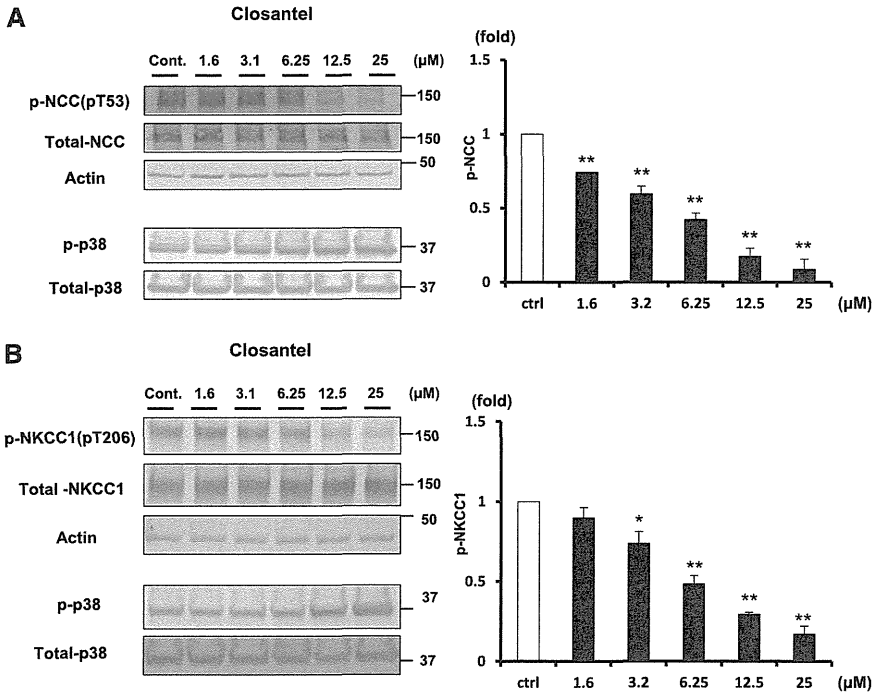


**Figure 9.** Inhibitory effect of Closantel on WNK-SPAK-NCC/NKCC1signaling in mpkDCT and MOVAS cells. (A) The left panel shows the inhibitory effect of Closantel in mpkDCT cells. The phosphorylation of NCC in mpkDCT cells is drastically and dose-dependently reduced by Closantel (1.6–25 $\mu$M). The right panel shows quantification of the results of the blots ($n$=4, mean±SEM). (B) The left panel shows the inhibitory effect of Closantel in MOVAS cells. The phosphorylation of NKCC1 is drastically and dose-dependently reduced by Closantel (1.6–25 $\mu$M). The right panel shows quantification of the results of the blots ($n$=4, mean±SEM). *$P$<0.05; **$P$<0.01. Cont/ctrl, control.

two hit compounds: 1S-14279 from a small-molecule compound library and Closantel from a library of existing drugs. Surprisingly, these two compounds had quite similar constitutions and both possessed strong SPAK inhibitory effects not only *in vitro* but also in cultured cell lines and in mice. Closantel is widely used as an antiparasitic agent in livestock either parenterally or orally at a single dose of 5–10 mg/kg. Some observations in humans for the treatment of liver fluke disease have been reported (E. Bernardiner, unpublished data). In recent years, the so-called drug repositioning strategy, in which an existing drug currently used for a specific disease is applied to another disease, has gained increasing attention from both academia and industry.[31] An advantage of this strategy is that existing drugs have already passed several stages of clinical development, which could reduce the development risk and costs. In this study, we identified a novel function of Closantel, which appeared to be less toxic than 1S-14279 because mice tolerated chronic treatment with Closantel, but not with 1S-14279. Closantel is a salicylanilide derivative that acts as an uncoupler of the oxidative phosphorylation in the cell mitochondria, which disturbs ATP production. However, in our study, another salicylanilide, oxyclozanide, had no SPAK inhibitory effect (data not shown). The compound structure of Closantel was quite important in the exertion of inhibitory actions on SPAK and the constitutional similarity of 1S-14279; Closantel may give us clues to the synthesis of compounds that have higher efficacy and less toxicity through further structural three-dimensional analysis.

It is noteworthy that both Closantel and 1S-14279 acted as non-ATP–competitive SPAK inhibitors. Most protein kinase inhibitors show an ATP-competitive type of kinase inhibition, which makes it difficult to determine high specificity because the human kinome is composed of >500 protein kinases that share a high degree of identity in the ATP binding pocket. Moreover, ATP-competitive inhibitors must compete with high intracellular ATP levels, leading to a discrepancy between $IC_{50}$ values measured during an *in vitro* study versus those measured during an *in vivo* study.[32] Thus, the ATP intensiveness of Closantel and 1S-14279 would be a clear advantage in generating highly specific inhibitors for SPAK.

In this study, we demonstrated that acute and chronic Closantel administration successfully decreased the expression of both phospho-NCC in the kidney and phospho-NKCC1 in the aorta. Similar results were observed in our previous studies with SPAK knockout mice.[17] After acute Closantel administration, the BP decreased very rapidly, suggesting that at least in the acute phase, the vasorelaxing effect of SPAK inhibition might be dominant over its natriuretic effect. Although heart rate also decreased, whether this resulted from specific SPAK inhibition and contributed to the decrease in BP requires further investigation. The involvement of SPAK in regulating intracellular $Na^+$ and $Cl^+$ in cardiomyocytes has been reported,[33,34] and an unidentified role of SPAK in the heart could be clarified by the discovery of SPAK inhibitors. Unfortunately, the natriuretic action of acute Closantel treatment could not be confirmed because we could not reproducibly collect urine samples in the short experimental period (the duration of activity of Closantel was too short to exert a diuretic effect; Supplemental Figure 3). In addition, we observed no significant increases in sodium excretion under chronic Closantel administration, although this may not be surprising given that SPAK knockout mice showed no such increase.[17] Experiments using larger animals and ureteric cannulation are necessary for detailed analysis of Closantel on kidney functions. Furthermore, hypertensive models are needed to assess the antihypertensive effect of Closantel, which may not have an effect on baseline BP like other antihypertensive drugs. Nevertheless, this study could clearly demonstrate that chronic Closantel treatment could inhibit SPAK.

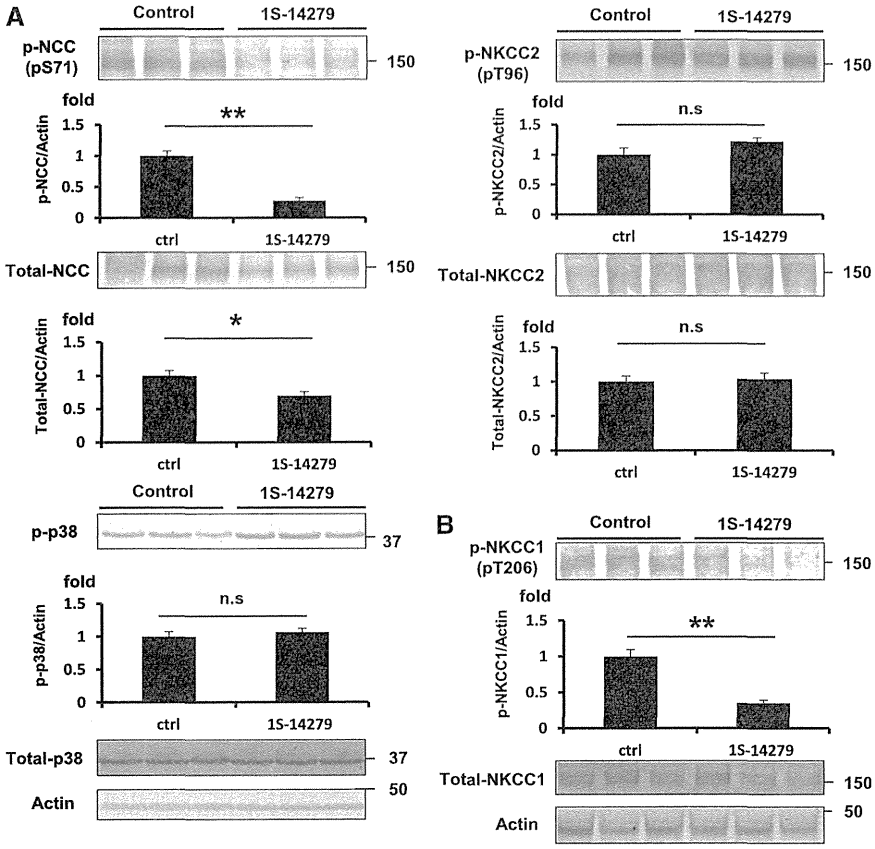


**Figure 10.** Inhibitory effect of 1S-14279 on WNK-SPAK-NCC/NKCC1 signaling in mouse kidney and aorta. (A) Representative immunoblots of total- and p-NCC, NKCC2, and p38 of the kidney at 30 minutes after infusion of 1S-14279. The NCC phosphorylation is drastically reduced by 1S-14279. No significant increases in pNKCC2 and p-p38 levels are observed. The lower panel shows quantification of the results of the blots ($n$=4, mean±SEM). (B) Representative immunoblots of total- and p-NKCC1 of the aorta at 30 minutes after infusion of 1S-14279. The expression of p-NKCC1 is markedly reduced. No significant difference in total NKCC1 abundance. The lower panel shows quantification of the results of the blots ($n$=4, mean±SEM). *$P$<0.05; **$P$<0.01. Ctrl, control.

Furthermore, OSR1 could also be inhibited by chronic Closantel treatment based on the observation that NKCC2 phosphorylation, which is mainly regulated by OSR1,[17] was decreased. This is plausible given that SPAK and OSR1 share high homology in their catalytic and regulatory domains.[17]

In conclusion, we found two hit compounds that inhibit SPAK kinase both *in vitro* and *in vivo*. Further pharmacologic modification of these compounds and their *in vivo* validation in other animal species and disease models could lead to the development of a novel antihypertensive drug.

## CONCISE METHODS

### Molecular Cloning and Plasmid Construction

The pRK5 expression plasmid containing T7-tagged whole SPAK was kindly provided by T. Moriguchi and H. Shibuya (Tokyo Medical and Dental University). The active SPAK [T233E] mutation[18] was introduced using the QuickChange Site-Directed Mutagenesis Kit (Agilent Technologies Inc., Santa Clara, CA) and cloned into the pGEX6p bacterial expression vector (GE Healthcare UK Ltd.). To clone human NKCC2 [1–174], RT-PCR was carried out using human kidney mRNA as a template, and the resulting PCR product was cloned into the pGEX6p bacterial expression vector. MO25$\alpha$ cDNA was generated by RT-PCR using mouse kidney mRNA as a template, and cloned into the pGEX6p expression vector.

### Expression of GST-Tagged Fusion Proteins in *Escherichia coli*

All recombinant GST fusion proteins were transformed into BL21 *E. coli* cells. One-liter cultures of the transformed *E. coli* were grown at 37°C in 2-YT broth containing 100 $\mu$g/ml ampicillin until the absorbance value at 600 nm reached 0.5. Isopropyl-D-galactosidase (0.2 mM) was then added to induce protein expression, and the cells were cultured for an additional 16 hours at 28°C. The cells were then collected by centrifugation at 4°C, lysed by sonication in 40 ml of ice-cold 1× PBS buffer containing Complete Protease Inhibitors (Roche Diagnostics), and incubated with 1% Triton X-100 and 0.5% salcosyl. The GST-tagged proteins were purified from the lysates using 1.2 ml of glutathione-Sepharose beads and eluted in an elution buffer containing 83 mM Tris-HCl, 150 mM KOH, and 30 mM glutathione.[26]

### Antibodies and Immunoblotting Analyses

Quantitative immunoblotting was performed as previously described.[4] Blots were probed with the following primary antibodies: anti-total NCC,[35] anti-phosphorylated NCC (pThr53 and pSer71 in mouse NCC),[11] anti-total NKCC1 (T4) (Hybridoma Bank, University of Iowa, Iowa City, IA), anti-phosphorylated NKCC1 (pThr206 in mouse NKCC1),[27] anti-total NKCC2 (Alpha Diagnostic, San Antonio, TX), anti-phosphorylated NKCC2 (pThr100 in human NKCC2),[36] anti-phosphorylated NKCC2 (termed pT2 antibody; kindly provided by K. Mutig),[37] anti-phosphorylated p38, anti-total p38 (Cell Signaling Technology, Danvers, MA), and anti-actin (Cytoskeleton, Denver, CO). Rabbit antiserum against phosphorylated NCC [residues 49–64 of mouse NCC phosphorylated at Thr53/58; Cys+LYMR(pT)FGYN (pT)IDVVPA] was generated and affinity purified. This antibody could be used to detect the phosphorylation of human NKCC2 at residues Thr100/105, which are equivalent to Thr55/60 in human NCC and Thr53/58 in mouse NCC. Alkaline phosphatase–conjugated anti-IgG antibodies (Promega, Madison, WI) were used as secondary antibodies and Western Blue (Promega) was used as a substrate for signal detection. The intensity of the bands was analyzed and quantified using ImageJ software (National Institutes of Health, Bethesda, MD).

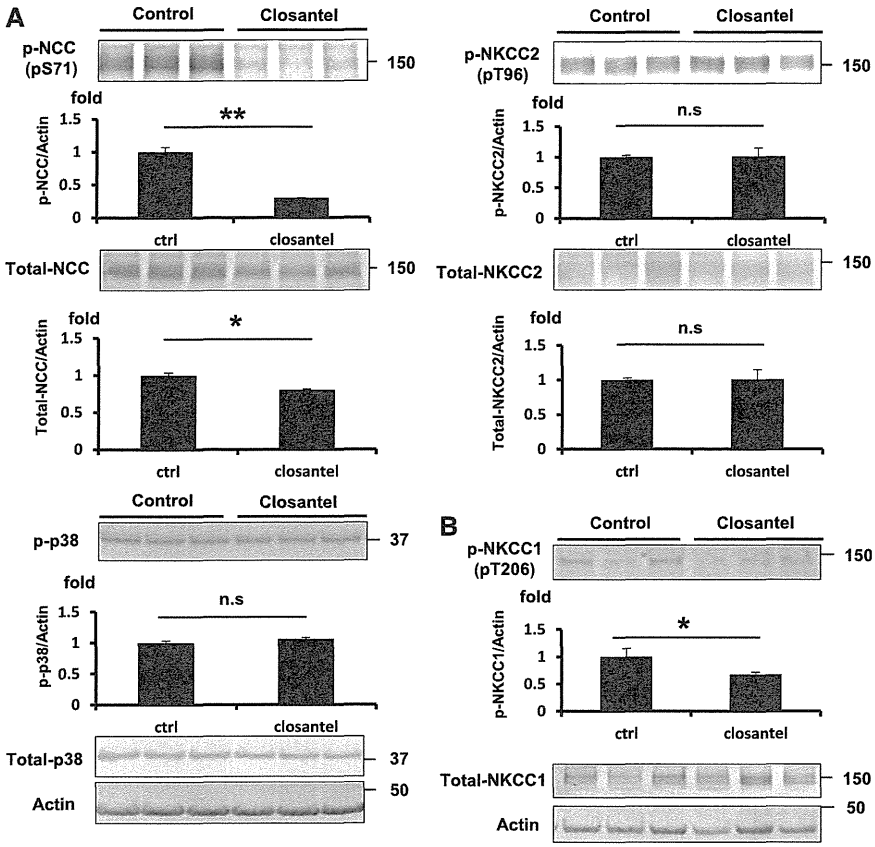


**Figure 11.** Inhibitory effect of Closantel on WNK-SPAK-NCC/NKCC1 signaling in mouse kidney and aorta. (A) Representative immunoblots of total- and p-NCC, NKCC2 and p38 of the kidney at 30 minutes after infusion of Closantel. The NCC phosphorylation is drastically reduced by Closantel. No significant increases in pNKCC2 and p-p38 levels are observed. The lower panel shows quantification of the results of the blots ($n$=3, mean±SEM). (B) Representative immunoblots of total- and p-NKCC1 of the aorta at 30 minutes after infusion of Closantel. The expression of p-NKCC1 is markedly reduced. No significant difference in total NKCC1 abundance. The lower panel shows quantification of the results of the blots ($n$=4, mean±SEM). *$P$<0.05; **$P$<0.01. Ctrl, control.

### *In Vitro* Kinase Assays

GST-NKCC1 [1–174] protein (7 $\mu$g) purified from *E. coli* was incubated with 1 $\mu$g of GST-SPAK [T233E] and 5 $\mu$g of GST-MO25$\alpha$. Kinase assay reactions were performed for 60 minutes at 30°C in a 25 $\mu$l of kinase reaction buffer (50 mM Tris-HCl [pH 7.5], 1 mM dithiothreitol, 1 mM EGTA) containing 10 mM $MgCl_2$ and 0.1 mM ATP as previously described.[6] The reactions were stopped by the addition of SDS sample buffer (Cosmo Bio Inc., Tokyo, Japan) followed by denaturation for 20 minutes at 60°C. The reaction products were analyzed by SDS-PAGE.

### Chemical Screening Using an Indirect ELISA System

GST-NKCC2 [1–174] (5 pmol/well) in a bicarbonate buffer (15 mM $Na_2CO_3$, 35 mM $NaHCO_3$) was applied to 96-well ELISA plates (Iwaki & Co., Ltd., Tokyo, Japan) and incubated overnight at 4°C for immobilization. After blocking with 1.5% (w/v) albumin in tris-buffered saline (TBS)-0.02% Tween 20 for 30 minutes at room temperature, kinase reactions were performed in 100 $\mu$l of kinase reaction buffer containing 10 mM $MgCl_2$, 0.1 mM ATP, 0.5 pmol of GST-SPAK [T233E], and 5 pmol of GST-MO25$\alpha$. After a 1-hour incubation at 30°C under gentle shaking, the plates were washed five times with wash buffer (TBS-0.02% Tween 20) using a Microplate Washer (ImmunoWash 1575; Bio-Rad, Mississauga, ON, Canada). Subsequently, 100 $\mu$l of 1.5 $\mu$g/ml rabbit anti-pNKCC2 antibody (pThr100/105; NCC pThr55/60) was applied to each well for the pNKCC2 assay and incubated overnight at 4°C. After washing, 100 $\mu$l of alkaline phosphatase–labeled anti-rabbit secondary antibody was added to each well and the plates were incubated for 1 hour at 37°C. After washing, 100 $\mu$l of BluePhos (KPL Inc., Gaithersburg, MD) was applied to each well, and the blue color developed was measured by reading the absorbance at 620 nm in a microplate reader (Spectrafluor; Tecan Japan Co., Ltd., Kanagawa, Japan). For chemical library screening, each compound was added to the kinase reaction at a final concentration of 50 $\mu$M. For inhibition studies, increasing concentrations of each compound were tested in triplicate. Curve fitting was performed using ORIGIN8.1 data analysis and graphing software (OriginLab Co., Ltd., Northampton, MA), and data are presented as the mean±SEM. Stock solutions of compounds, in 100% DMSO, were diluted with water to a final DMSO concentration of 1%. Controls without inhibitors were also incubated in the presence of 1% DMSO.

### Kinetic Binding Analyses Using a Biacore Biosensor

The binding kinetics between SPAK and the various compounds were analyzed using a Biacore T100 system (GE Healthcare UK Ltd.). CM5 sensor chips were docked and GST-SPAK [T233E] was injected for 7 minutes at a flow rate of 10 $\mu$l/min over the surface after preactivation with a mixture of 0.2 M 1-ethyl-3-[3-dimethylaminopropyl]carbodiimide hydrochloride and 0.05 M sulfo-*N*-hydroxysuccinimide. After the injection of GST-SPAK [T233E], the surface was deactivated with 150 $\mu$l of 1 M ethanolamine HCl (pH 8.5), giving an immobilization level for GST-SPAK [T233E] of approximately 10,000 resonance units. To reduce nonspecific binding, we used a reference surface immobilized with GST at 3000 resonance units. The TBS-based buffer (50 mM Tris-HCl [pH 7.5], 150 mM NaCl, 10 mM $MgCl_2$, 0.05% surfactant-P) with 5% DMSO was used as a running buffer to facilitate dissolution of the compounds, and the temperature was set to 25°C. Analysis of the interactions between the small-molecule compounds and GST-SPAK [T233E] was carried out using a one-shot kinetic approach. For each compound, a series of solutions of four different concentrations and a blank sample for double referencing were injected for 60 seconds at a flow rate of 90 $\mu$l/min. No regeneration was applied. The sensorgrams

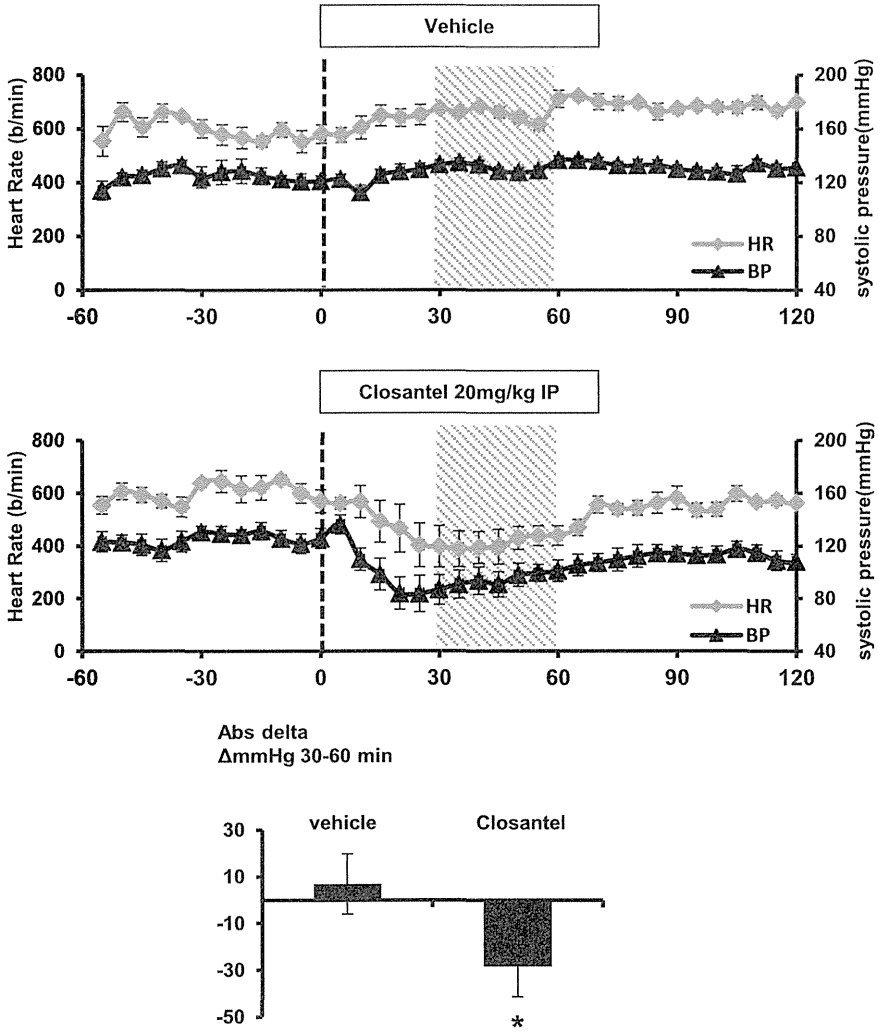


**Figure 12.** Acute Closantel administration-induced hypotension in mice. The line graphs represent the systolic arterial BP (black triangles; $n$=5) and heart rate (gray diamonds; $n$=5) before and after vehicle (40% DMSO) and Closantel (20 mg/kg in 40% DMSO) administration. The dashed vertical lines indicate the beginning of drug administration. The shaded area represents the period under analysis. The bar graphs show the average decrease in systolic arterial pressure during the 30- to 60-minute postinjection period (*$P$<0.05; $n$=5, mean±SEM). Closantel induces a marked reduction in the BP, which appears to precede the decrease in the heart rate, and persists longer. HR, heart rate; IP, intraperitoneal; Ab, antibody.

were processed and fitted to determine the dissociation constants using Biacore T100 evaluation software.

## Kinase Profiling

Kinase profiling was conducted by PerkinElmer (Boston, MA) using a RapidKinase48 panel in duplicate wells. The compounds were tested at a final concentration of 1.0E-5 (M). Each test compound was incubated with each of the kinases and appropriate substrates according to PerkinElmer standard operating procedures. After the incubation period, the reaction products and remaining substrate were measured. According to PerkinElmer guidelines, compounds that show ≥50% inhibition are considered active.

## Cell Culture and Inhibition Assay

The mpkDCT cell line kindly provided by A. Vandewalle was cultured in a defined medium as previously described.[38] MOVAS cells were cultured in DMEM supplemented with 10% (v/v) FBS, 2 mM L-glutamine, 100 U/ml penicillin, and 0.1 mg/ml streptomycin at 37°C in a humidified 5% $CO_2$ incubator. mpkDCT and MOVAS cells were cultured on six-well dishes. Hypotonic stimulation was performed as previously reported.[26] For the inhibition assay, cells were exposed to each compound for 30 minutes and then stimulated with a hypotonic low-chloride medium for 30 minutes.[25] Cells were then lysed in 0.15 ml of ice-cold cell lysis buffer (50 mM Tris-HCl [pH 7.5], 150 mM NaCl, 1 mM EGTA, 1 mM EDTA, 50 mM sodium fluoride, 1 mM sodium orthovanadate, 1% Triton X-100, 0.27 M sucrose, 1 mM dithiothreitol) per well. After centrifugation at 12,000×$g$ for 5 minutes at 4°C, the supernatants were denatured for 20 minutes at 60°C with SDS sample buffer and subjected to SDS-PAGE.

## Animal Studies

Female C57BL/6 mice (10 weeks old) were obtained and received standard laboratory chow and water. The Animal Care and Use Committee of Tokyo Medical and Dental University approved the experimental protocol. In an acute treatment study, 1S-14279 and Closantel were both administered intraperitoneally at a dose of 20 mg/kg in 40 $\mu$l of DMSO; the control mice were administered 40 $\mu$l of DMSO alone. The mice were euthanized 30 minutes after injection. In the chronic treatment study, C57BL/6 mice were fed the mouse chow containing Closantel at a dosage of 300 mg/kg per day. The kidney was removed and rapidly homogenized in a 10-fold mass excess of ice-cold 1% (w/v) Triton X-100 lysis buffer. Whole homogenates without the nuclear fraction (600×$g$) were collected and denatured at 60°C for 20 minutes as previously reported.[4] The aorta was rapidly isolated and frozen with liquid nitrogen. After being crushed by sonication, aortas were added to 150 $\mu$l of lysis buffer as previously reported,[7] and centrifuged at 6000×$g$ for 5 minutes at 4°C. A 120-$\mu$l aliquot of the supernatant was denatured at 60°C for 20 minutes. The total protein concentration was determined by the Bradford method using BSA as a standard, and lysates were stored at −80°C. Quantitative immunoblotting was performed as previously described.[12] The relative intensities of immunoblot bands were determined by densitometry using ImageJ software.

The BP of the mice was measured using a radiotelemetric method in which a BP transducer (Data Sciences International, St. Paul, MN) was inserted into the left carotid artery. The mice were housed individually

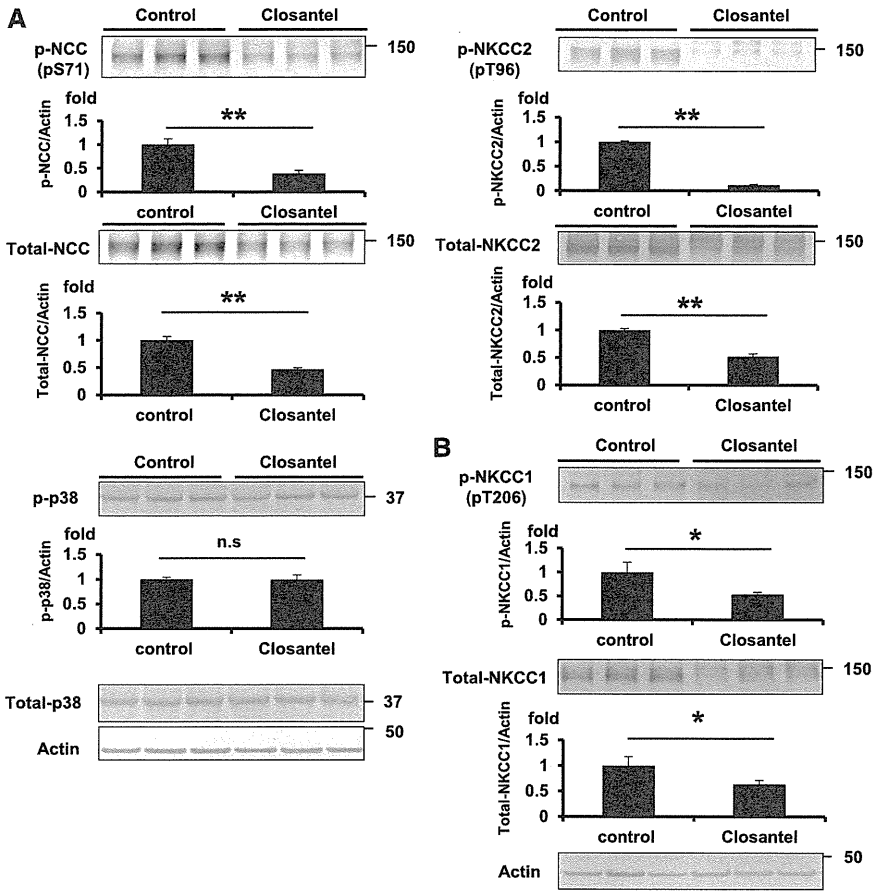


**Figure 13.** Inhibitory effect of chronic Closantel treatment on WNK-SPAK-NCC/NKCC1 signaling in mouse kidney and aorta. The dosage of Closantel added to the mouse chow is 300 mg/kg per day. (A) Representative immunoblots of total- and p-NCC and NKCC2 after 7 days treatment of Closantel. NCC and NKCC2 phosphorylation are markedly reduced by Closantel. The lower panel shows the quantification of the results of the blots ($n$=4, mean±SEM). (B) Representative immunoblots for the total- and p-NKCC1 of the aorta after 7 days Closantel administration. The expression of p-NKCC1 is markedly reduced. The lower panel shows the quantification of the results of the blots ($n$=4, mean±SEM). *$P$<0.05; **$P$<0.01.

in a standard cage with a 12-hour/12-hour light/dark cycle and received standard laboratory chow and water as previously described.[39] Seven days after transplantation, the systolic and diastolic arterial pressures were recorded 1 hour before and 2 hours after intraperitoneal injections of either 20 mg/kg Closantel dissolved in 40% DMSO or 40% DMSO alone as a vehicle control. All drugs were freshly prepared in DMSO each day, and the effect of each drug or vehicle was assessed on separate days. Blood was drawn from the retro-orbital sinus under light ether anesthesia. Serum data were determined using the i-STAT system (FUSO Pharmaceutical Industries, Osaka, Japan). Urine electrolytes were determined using a Fuji DRI-CHEM 4000 system (FujiFilm, Tokyo, Japan). Serum and urine creatinine concentrations were determined using a commercial kit (LabAssay Creatinine; Wako Chemical Inc., Osaka, Japan).

### Statistical Analyses

Data are expressed as the mean±SEM. Comparisons between the two groups were performed with unpaired $t$ tests. $P$ values <0.05 were considered statistically significant.

## ACKNOWLEDGMENTS

We thank Makiko Nawa (Laboratory of Cytometry and Proteome Research, Tokyo Medical and Dental University) for her help with Biacore analysis. We also thank Dr. K. Mutig and A. Vandewalle for the provision of pT2 antibody and mpkDCT cells, respectively.

This study was supported in part by Grants-in-Aid for Scientific Research (S) and (A) from the Japan Society for the Promotion of Science; a Grant-in-Aid for Young Scientists (B) from the Ministry of Education, Culture, Sports, Science and Technology of Japan; a Health and Labor Sciences Research Grant from the Ministry of Health, Labor and Welfare of Japan; and grants from the Salt Science Research Foundation (no. 1422), the Takeda Science Foundation, the Banyu Foundation, and the Vehicle Racing Commemorative Foundation.

## DISCLOSURES

None.

## REFERENCES

1. Shimkets RA, Warnock DG, Bositis CM, Nelson-Williams C, Hansson JH, Schambelan M, Gill JR Jr, Ulick S, Milora RV, Findling JW, Canessa CM, Rossier BC, Lifton RP: Liddle's syndrome: Heritable human hypertension caused by mutations in the beta subunit of the epithelial sodium channel. *Cell* 79: 407–414, 1994
2. Achard JM, Disse-Nicodeme S, Fiquet-Kempf B, Jeunemaitre X: Phenotypic and genetic heterogeneity of familial hyperkalaemic hypertension (Gordon syndrome). *Clin Exp Pharmacol Physiol* 28: 1048–1052, 2001
3. Wilson FH, Disse-Nicodème S, Choate KA, Ishikawa K, Nelson-Williams C, Desitter I, Gunel M, Milford DV, Lipkin GW, Achard JM, Feely MP, Dussol B, Berland Y, Unwin RJ, Mayan H, Simon DB, Farfel Z, Jeunemaitre X, Lifton RP: Human hypertension caused by mutations in WNK kinases. *Science* 293: 1107–1112, 2001
4. Yang SS, Morimoto T, Rai T, Chiga M, Sohara E, Ohno M, Uchida K, Lin SH, Moriguchi T, Shibuya H, Kondo Y, Sasaki S, Uchida S: Molecular pathogenesis of pseudohypoaldosteronism type II: Generation and analysis of a Wnk4(D561A/+) knockin mouse model. *Cell Metab* 5: 331–344, 2007
5. Wakabayashi M, Mori T, Isobe K, Sohara E, Susa K, Araki Y, Chiga M, Kikuchi E, Nomura N, Mori Y, Matsuo H, Murata T, Nomura S, Asano T, Kawaguchi H, Nonoyama S, Rai T, Sasaki S, Uchida S: Impaired KLHL3-mediated ubiquitination of WNK4 causes human hypertension. *Cell Reports* 3: 858–868, 2013
6. Richardson C, Rafiqi FH, Karlsson HK, Moleleki N, Vandewalle A, Campbell DG, Morrice NA, Alessi DR: Activation of the thiazide-sensitive Na+-Cl- cotransporter by the WNK-regulated kinases SPAK and OSR1. *J Cell Sci* 121: 675–684, 2008
7. Zeniya M, Sohara E, Kita S, Iwamoto T, Susa K, Mori T, Oi K, Chiga M, Takahashi D, Yang SS, Lin SH, Rai T, Sasaki S, Uchida S: Dietary salt

intake regulates WNK3-SPAK-NKCC1 phosphorylation cascade in mouse aorta through angiotensin II. *Hypertension* 62: 872–878, 2013
8. Meyer JW, Flagella M, Sutliff RL, Lorenz JN, Nieman ML, Weber CS, Paul RJ, Shull GE: Decreased blood pressure and vascular smooth muscle tone in mice lacking basolateral Na(+)-K(+)-2Cl(-) cotransporter. *Am J Physiol Heart Circ Physiol* 283: H1846–H1855, 2002
9. Akar F, Jiang G, Paul RJ, O'Neill WC: Contractile regulation of the Na (+)-K(+)-2Cl(-) cotransporter in vascular smooth muscle. *Am J Physiol Cell Physiol* 281: C579–C584, 2001
10. Garg P, Martin CF, Elms SC, Gordon FJ, Wall SM, Garland CJ, Sutliff RL, O'Neill WC: Effect of the Na-K-2Cl cotransporter NKCC1 on systemic blood pressure and smooth muscle tone. *Am J Physiol Heart Circ Physiol* 292: H2100–H2105, 2007
11. Chiga M, Rai T, Yang SS, Ohta A, Takizawa T, Sasaki S, Uchida S: Dietary salt regulates the phosphorylation of OSR1/SPAK kinases and the sodium chloride cotransporter through aldosterone. *Kidney Int* 74: 1403–1409, 2008
12. Sohara E, Rai T, Yang SS, Ohta A, Naito S, Chiga M, Nomura N, Lin SH, Vandewalle A, Ohta E, Sasaki S, Uchida S: Acute insulin stimulation induces phosphorylation of the Na-Cl cotransporter in cultured distal mpkDCT cells and mouse kidney. *PLoS ONE* 6: e24277, 2011
13. Nishida H, Sohara E, Nomura N, Chiga M, Alessi DR, Rai T, Sasaki S, Uchida S: Phosphatidylinositol 3-kinase/Akt signaling pathway activates the WNK-OSR1/SPAK-NCC phosphorylation cascade in hyperinsulinemic db/db mice. *Hypertension* 60: 981–990, 2012
14. Talati G, Ohta A, Rai T, Sohara E, Naito S, Vandewalle A, Sasaki S, Uchida S: Effect of angiotensin II on the WNK-OSR1/SPAK-NCC phosphorylation cascade in cultured mpkDCT cells and in vivo mouse kidney. *Biochem Biophys Res Commun* 393: 844–848, 2010
15. Castañeda-Bueno M, Cervantes-Pérez LG, Vázquez N, Uribe N, Kantesaria S, Morla L, Bobadilla NA, Doucet A, Alessi DR, Gamba G: Activation of the renal Na+:Cl- cotransporter by angiotensin II is a WNK4-dependent process. *Proc Natl Acad Sci U S A* 109: 7929–7934, 2012
16. Chiga M, Rafiqi FH, Alessi DR, Sohara E, Ohta A, Rai T, Sasaki S, Uchida S: Phenotypes of pseudohypoaldosteronism type II caused by the WNK4 D561A missense mutation are dependent on the WNK-OSR1/SPAK kinase cascade. *J Cell Sci* 124: 1391–1395, 2011
17. Yang SS, Lo YF, Wu CC, Lin SW, Yeh CJ, Chu P, Sytwu HK, Uchida S, Sasaki S, Lin SH: SPAK-knockout mice manifest Gitelman syndrome and impaired vasoconstriction. *J Am Soc Nephrol* 21: 1868–1877, 2010
18. Filippi BM, de los Heros P, Mehellou Y, Navratilova I, Gourlay R, Deak M, Plater L, Toth R, Zeqiraj E, Alessi DR: MO25 is a master regulator of SPAK/OSR1 and MST3/MST4/YSK1 protein kinases. *EMBO J* 30: 1730–1741, 2011
19. Vitari AC, Deak M, Morrice NA, Alessi DR: The WNK1 and WNK4 protein kinases that are mutated in Gordon's hypertension syndrome phosphorylate and activate SPAK and OSR1 protein kinases. *Biochem J* 391: 17–24, 2005
20. Zagórska A, Pozo-Guisado E, Boudeau J, Vitari AC, Rafiqi FH, Thastrup J, Deak M, Campbell DG, Morrice NA, Prescott AR, Alessi DR: Regulation of activity and localization of the WNK1 protein kinase by hyperosmotic stress. *J Cell Biol* 176: 89–100, 2007
21. Karaman MW, Herrgard S, Treiber DK, Gallant P, Atteridge CE, Campbell BT, Chan KW, Ciceri P, Davis MI, Edeen PT, Faraoni R, Floyd M, Hunt JP, Lockhart DJ, Milanov ZV, Morrison MJ, Pallares G, Patel HK, Pritchard S, Wodicka LM, Zarrinkar PP: A quantitative analysis of kinase inhibitor selectivity. *Nat Biotechnol* 26: 127–132, 2008
22. Gagnon KB, England R, Delpire E: Characterization of SPAK and OSR1, regulatory kinases of the Na-K-2Cl cotransporter. *Mol Cell Biol* 26: 689–698, 2006
23. Butini S, Gemma S, Brindisi M, Borrelli G, Lossani A, Ponte AM, Torti A, Maga G, Marinelli L, La Pietra V, Fiorini I, Lamponi S, Campiani G, Zisterer DM, Nathwani SM, Sartini S, La Motta C, Da Settimo F, Novellino E, Focher F: Non-nucleoside inhibitors of human adenosine kinase: Synthesis, molecular modeling, and biological studies. *J Med Chem* 54: 1401–1420, 2011
24. Koltsova SV, Kotelevtsev SV, Tremblay J, Hamet P, Orlov SN: Excitation-contraction coupling in resistance mesenteric arteries: Evidence for NKCC1-mediated pathway. *Biochem Biophys Res Commun* 379: 1080–1083, 2009
25. Naito S, Ohta A, Sohara E, Ohta E, Rai T, Sasaki S, Uchida S: Regulation of WNK1 kinase by extracellular potassium. *Clin Exp Nephrol* 15: 195–202, 2011
26. Mori T, Kikuchi E, Watanabe Y, Fujii S, Ishigami-Yuasa M, Kagechika H, Sohara E, Rai T, Sasaki S, Uchida S: Chemical library screening for WNK signalling inhibitors using fluorescence correlation spectroscopy. *Biochem J* 455: 339–345, 2013
27. Lin SH, Yu IS, Jiang ST, Lin SW, Chu P, Chen A, Sytwu HK, Sohara E, Uchida S, Sasaki S, Yang SS: Impaired phosphorylation of Na(+)-K (+)-2Cl(-) cotransporter by oxidative stress-responsive kinase-1 deficiency manifests hypotension and Bartter-like syndrome. *Proc Natl Acad Sci U S A* 108: 17538–17543, 2011
28. Uchida S: Pathophysiological roles of WNK kinases in the kidney. *Pflugers Arch* 460: 695–702, 2010
29. Kahle KT, Rinehart J, Giebisch G, Gamba G, Hebert SC, Lifton RP: A novel protein kinase signaling pathway essential for blood pressure regulation in humans. *Trends Endocrinol Metab* 19: 91–95, 2008
30. Richardson C, Alessi DR: The regulation of salt transport and blood pressure by the WNK-SPAK/OSR1 signalling pathway. *J Cell Sci* 121: 3293–3304, 2008
31. Ashburn TT, Thor KB: Drug repositioning: Identifying and developing new uses for existing drugs. *Nat Rev Drug Discov* 3: 673–683, 2004
32. Garuti L, Roberti M, Bottegoni G: Non-ATP competitive protein kinase inhibitors. *Curr Med Chem* 17: 2804–2821, 2010
33. Pedersen SF, O'Donnell ME, Anderson SE, Cala PM: Physiology and pathophysiology of Na+/H+ exchange and Na+ -K+ -2Cl- cotransport in the heart, brain, and blood. *Am J Physiol Regul Integr Comp Physiol* 291: R1–R25, 2006
34. Bers DM, Barry WH, Despa S: Intracellular Na+ regulation in cardiac myocytes. *Cardiovasc Res* 57: 897–912, 2003
35. Ohno M, Uchida K, Ohashi T, Nitta K, Ohta A, Chiga M, Sasaki S, Uchida S: Immunolocalization of WNK4 in mouse kidney. *Histochem Cell Biol* 136: 25–35, 2011
36. Richardson C, Sakamoto K, de los Heros P, Deak M, Campbell DG, Prescott AR, Alessi DR: Regulation of the NKCC2 ion cotransporter by SPAK-OSR1-dependent and -independent pathways. *J Cell Sci* 124: 789–800, 2011
37. Mutig K, Paliege A, Kahl T, Jöns T, Müller-Esterl W, Bachmann S: Vasopressin V2 receptor expression along rat, mouse, and human renal epithelia with focus on TAL. *Am J Physiol Renal Physiol* 293: F1166–F1177, 2007
38. Diepens RJ, den Dekker E, Bens M, Weidema AF, Vandewalle A, Bindels RJ, Hoenderop JG: Characterization of a murine renal distal convoluted tubule cell line for the study of transcellular calcium transport. *Am J Physiol Renal Physiol* 286: F483–F489, 2004
39. Susa K, Kita S, Iwamoto T, Yang SS, Lin SH, Ohta A, Sohara E, Rai T, Sasaki S, Alessi DR, Uchida S: Effect of heterozygous deletion of WNK1 on the WNK-OSR1/ SPAK-NCC/NKCC1/NKCC2 signal cascade in the kidney and blood vessels. *Clin Exp Nephrol* 16: 530–538, 2012

This article contains supplemental material online at http://jasn.asnjournals.org/lookup/suppl/doi:10.1681/ASN.2014060560/-/DCSupplemental.

BASIC RESEARCH www.jasn.org

# Kelch-Like Protein 2 Mediates Angiotensin II–With No Lysine 3 Signaling in the Regulation of Vascular Tonus

Moko Zeniya, Nobuhisa Morimoto, Daiei Takahashi, Yutaro Mori, Takayasu Mori, Fumiaki Ando, Yuya Araki, Yuki Yoshizaki, Yuichi Inoue, Kiyoshi Isobe, Naohiro Nomura, Katsuyuki Oi, Hidenori Nishida, Sei Sasaki, Eisei Sohara, Tatemitsu Rai, and Shinichi Uchida

Department of Nephrology, Graduate School of Medical and Dental Sciences, Tokyo Medical and Dental University, Tokyo, Japan

## ABSTRACT

Recently, the kelch-like protein 3 (KLHL3)–Cullin3 complex was identified as an E3 ubiquitin ligase for with no lysine (WNK) kinases, and the impaired ubiquitination of WNK4 causes pseudohypoaldosteronism type II (PHAII), a hereditary hypertensive disease. However, the involvement of WNK kinase regulation by ubiquitination in situations other than PHAII has not been identified. Previously, we identified the WNK3–STE20/SPS1-related proline/alanine-rich kinase–Na/K/Cl cotransporter isoform 1 phosphorylation cascade in vascular smooth muscle cells and found that it constitutes an important mechanism of vascular constriction by angiotensin II (AngII). In this study, we investigated the involvement of KLHL proteins in AngII-induced WNK3 activation of vascular smooth muscle cells. In the mouse aorta and mouse vascular smooth muscle (MOVAS) cells, KLHL3 was not expressed, but KLHL2, the closest homolog of KLHL3, was expressed. Salt depletion and acute infusion of AngII decreased KLHL2 and increased WNK3 levels in the mouse aorta. Notably, the AngII-induced changes in KLHL2 and WNK3 expression occurred within minutes in MOVAS cells. Results of KLHL2 overexpression and knockdown experiments in MOVAS cells confirmed that KLHL2 is the major regulator of WNK3 protein abundance. The AngII-induced decrease in KLHL2 was not caused by decreased transcription but increased autophagy-mediated degradation. Furthermore, knockdown of sequestosome 1/p62 prevented the decrease in KLHL2, suggesting that the mechanism of KLHL2 autophagy could be selective autophagy mediated by sequestosome 1/p62. Thus, we identified a novel component of signal transduction in AngII-induced vascular contraction that could be a promising drug target.

*J Am Soc Nephrol* 26: ●●●–●●●, 2015. doi: 10.1681/ASN.2014070639

Recently, the kelch-like protein 3 (KLHL3) and Cullin3 (Cul3) were identified as the genes responsible for a hereditary hypertensive disease—pseudohypoaldosteronism type II (PHAII).[1] Because the with no lysine (WNK) kinases (WNK1 and WNK4) had already been identified as the responsible genes for PHAII and the KLHL proteins were known to serve as substrate adaptors of Cul3-based E3 ubiquitin ligase,[1–3] we speculated and recently showed that KLHL3 functions as an E3 ligase with Cul3 for WNK4 and that the impaired ubiquitination of WNK4 and its subsequent increase within the cell stimulates the downstream OSR1/STE20/SPS1-related proline/alanine-rich kinase (SPAK)–NaCl cotransporter signaling and causes PHAII.[4] In addition to WNK4, WNK1 and other WNK kinases (WNK2 and WNK3) have been identified as substrates of KLHL3–Cul3 E3 ligase, because KLHL3 can bind to all WNKs in a highly conserved domain (acidic domain).[5] Furthermore, we recently reported that KLHL2 possesses a kelch repeat domain (WNK binding domain) highly similar to that of KLHL3 and that

Received July 2, 2014. Accepted October 21, 2014.

Published online ahead of print. Publication date available at www.jasn.org.

**Correspondence:** Prof. Shinichi Uchida, 1-5-45 Yushima, Bunkyo, Tokyo 113-8519, Japan. Email: suchida.kid@tmd.ac.jp

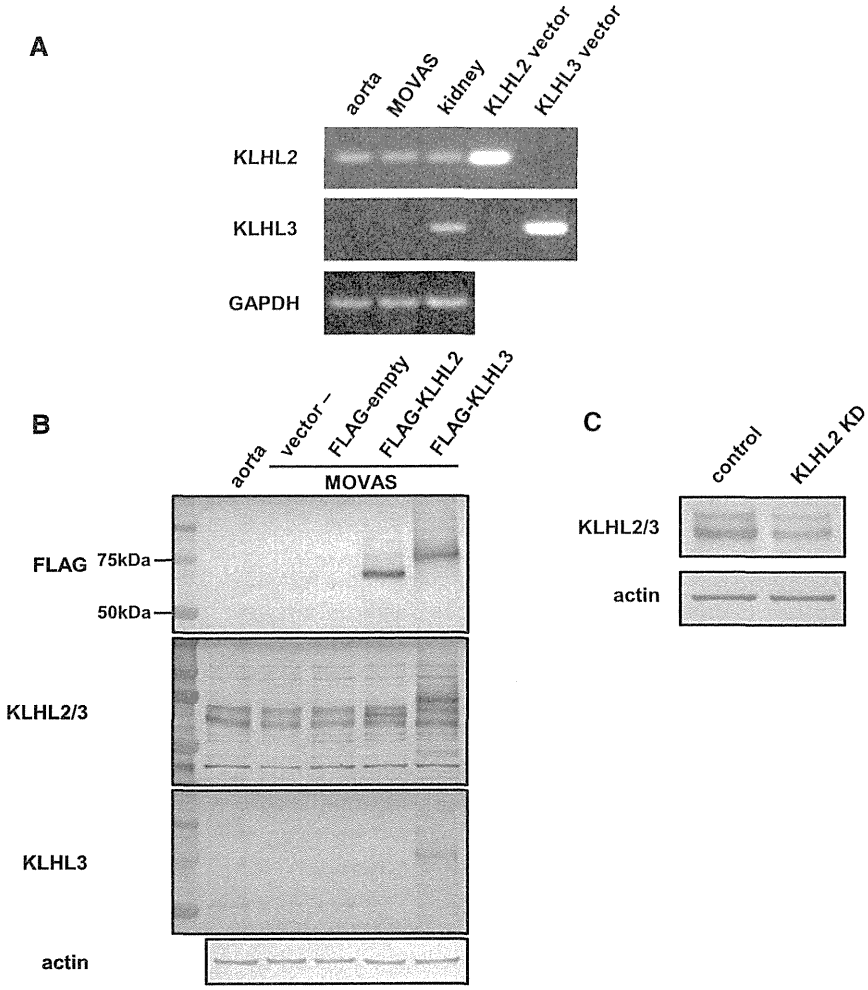


**Figure 1.** KLHL2 and not KLHL3 is expressed in mouse aorta and MOVAS cells. (A) Expression of KLHL2 and KLHL3 in the mouse aorta and MOVAS cells was investigated by RT-PCR. KLHL2 was expressed in the mouse aorta and MOVAS cells, although KLHL3 mRNA was not detected. (B) Immunoblots of KLHL2 and KLHL3 in the mouse aorta and MOVAS cells. 3XFLAG-tagged KLHL2 and KLHL3 that were overexpressed in MOVAS cells were used as controls. The anti-KLHL2/KLHL3 antibody recognized both 3XFLAG-tagged KLHL2 and KLHL3 and detected double bands around 65 kD in the aorta and MOVAS cells. The anti-KLHL3 antibody recognized only 3XFLAG KLHL3 but detected no band in the aorta and MOVAS cells. (C) Immunoblot with the anti-KLHL2/KLHL3 antibody in KLHL2 knockdown MOVAS cells. The KLHL2 knockdown by siRNA decreased both bands. GAPDH, glyceraldehyde-3-phosphate dehydrogenase

KLHL2–Cul3 also functions as an E3 ligase for all WNK kinases.[6] These data strongly suggest that any combination of KLHL2/KLHL3 with WNK1/WNK2/WNK3/WNK4 could occur in various types of cells and that KLHL-mediated regulation of WNK kinase abundance by ubiquitination could be involved in the mechanisms of WNK kinase regulation under various pathophysiologic conditions other than PHAII. To date, we have identified several upstream regulators for WNK kinases, including hormonal factors, such as aldosterone, angiotensin II (AngII), insulin, and vasopressin.[7–11] However, the mechanisms of signal transduction from these factors to WNK kinases have not necessarily been clarified. We speculated that one of these regulations could be mediated by the ubiquitination of WNKs by KLHL2 and/or KLHL3.

We recently identified WNK3–SPAK–Na/K/Cl cotransporter isoform 1 (NKCC1) signaling in mouse arteries, which plays an important role in the regulation of vascular smooth muscle cell contractions with AngII.[12] Influx of $Cl^-$ through NKCC1 changes membrane depolarization and leads to voltage-gated Ca channel activation, which causes the elevation of peripheral resistance.[13] SPAK regulates NKCC1 activity by its phosphorylation in its amino terminal domain,[14] and SPAK is regulated by the phosphorylation by WNK3 as well as WNK1.[15] Although we have clarified that WNK3 is necessary for SPAK–NKCC1 activation by AngII using WNK3 knockout mice, little is known about how AngII activates WNK3–SPAK–NKCC1 signaling.

In this study, we identified that KLHL2 and not KLHL3 was expressed in mouse aorta and vascular smooth muscle cells. We also showed that AngII rapidly decreased KLHL2 protein abundance, thereby causing the increase in WNK3 and its downstream activation. Interestingly, the rapid decrease in KLHL2 by AngII was mediated by autophagy-mediated degradation of KLHL2, which could be a novel mechanism in KLHL and WNK regulations as well as AngII-induced signal transduction.

## RESULTS

### KLHL2 and Not KLHL3 Is Expressed in the Mouse Aorta and Mouse Vascular Smooth Muscle Cells

We have reported that KLHL2 is the closest homolog to KLHL3 among >40 members of the KLHL proteins and that KLHL2 could interact with all WNK kinases, including WNK3.[6] Furthermore, WNK3 showed the highest binding affinity with KLHL2 and KLHL3 among the WNK kinases, suggesting that WNK3 as well as WNK4 could be regulated by KLHL2 or KLHL3 in its signaling cascade.[6] To investigate the role of KLHL2 and KLHL3 in WNK3 signaling in vascular smooth muscle cells, we first examined whether KLHL2 and KLHL3 were expressed in the mouse aorta and mouse vascular smooth muscle (MOVAS) cells by RT-PCR. As shown in Figure 1A, KLHL2 was expressed in the mouse aorta and MOVAS cells; however, KLHL3 mRNA was not detected. In the immunoblots of aorta and MOVAS cells, the anti-KLHL2/KLHL3 antibody detected double bands around 65 kD, whereas the KLHL3-specific antibody did not detect any signal (Figure 1B). The KLHL2 knockdown by siRNA decreased

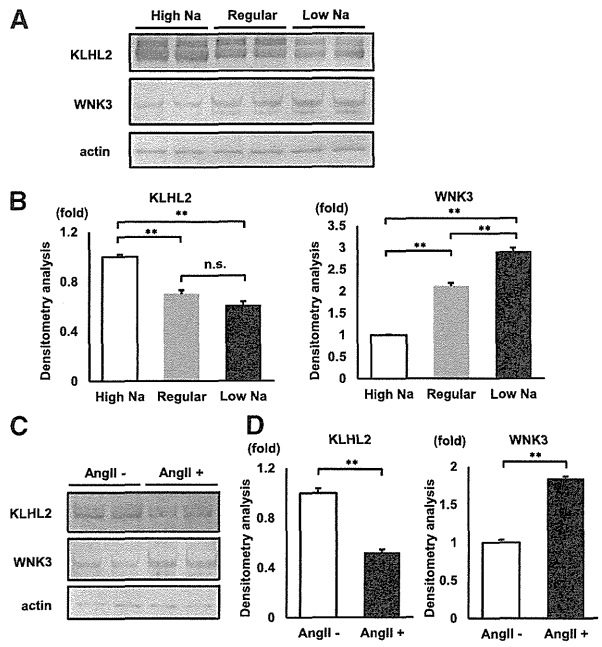


**Figure 2.** Dietary salt and acute AngII infusion decrease KLHL2 and increase WNK3 in mouse aorta. (A) Representative immunoblots and (B) densitometry analyses ($n$=6) of KLHL2 and WNK3 in aortas from mice fed high-, normal-, and low-salt diets. KLHL2 in mouse aorta was decreased by a low-salt diet and increased by a high-salt diet. WNK3 in the mouse aorta was increased by a low-salt diet and decreased by a high-salt diet. (C) Representative immunoblots and (D) densitometry analyses ($n$=4) of KLHL2 and WNK3 in aortas from mice at 30 minutes after AngII infusion. Acute AngII infusion decreased KLHL2 and increased WNK3. $^{**}P<0.01$.

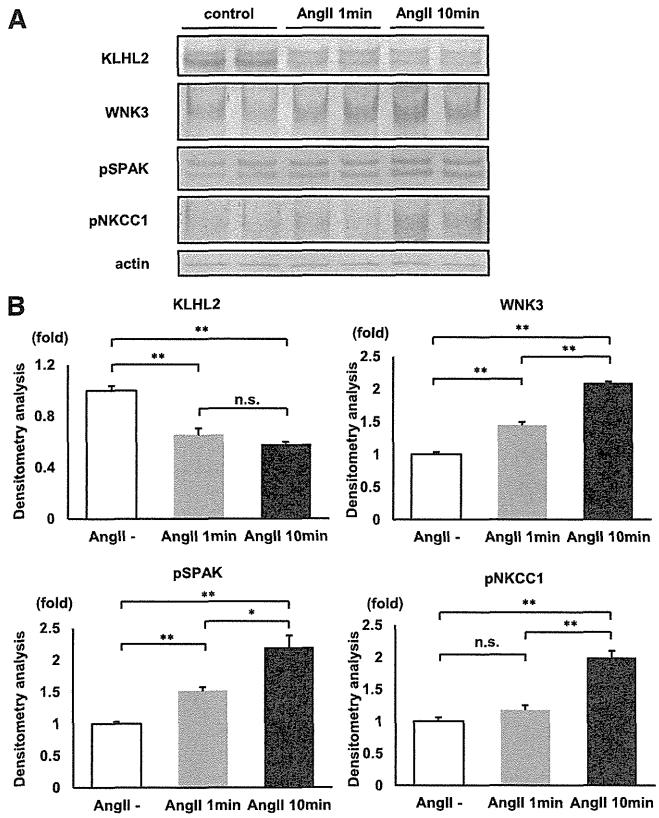


**Figure 3.** AngII rapidly decreases KLHL2 and increases WNK3–SPAK–NKCC1 phosphorylation cascade in MOVAS cells. (A) Representative immunoblots and (B) densitometry analyses ($n$=5) of KLHL2, WNK3, phosphorylated SPAK (pSPAK), and phosphorylated NKCC1 (pNKCC1) in MOVAS cells treated by AngII. In 1 minute after AngII treatment, KLHL2 was decreased, and the WNK3–SPAK–NKCC1 phosphorylation cascade was activated. After 10 minutes, the tendency was more prominent. $^{*}P<0.05$; $^{**}P<0.01$.

both bands detected by the anti-KLHL2/KLHL3 antibody (Figure 1C). On the basis of these data, we concluded that the double bands detected by the anti-KLHL2/KLHL3 antibody in the mouse aorta and MOVAS cells were KLHL2. The lower band may be the major KLHL2 band that corresponds to cloned KLHL2 cDNA because the overexpressed KLHL2 had a 3XFLAG tag (Figure 1B). Although the nature of the upper band remains to be determined, we can exclude the possibility of protein modifications by phosphorylation, glycosylation, and neddylation by the experiments using phosphatase, glycosidase, and MLN4924 (data not shown). With these results, we focused on KLHL2 in WNK3 regulation in the mouse aorta and MOVAS cells.

### Salt Depletion and Acute AngII Infusion Decrease KLHL2 and Increase WNK3 in the Mouse Aorta

We have reported that the regulation of the WNK3–SPAK–NKCC1 phosphorylation cascade by AngII in arteries is important for the maintenance of BP in cases of salt depletion.[12] However, how AngII regulated WNK3 remains unclear. Previously, we could not detect WNK3 protein in the mouse aorta with any WNK3 antibodies that were available at that time. However, we have recently improved the method of detecting the WNK3 protein in tiny mouse aortic tissues (Supplemental Figure 1). As shown in Figure 2, A and B, a high-salt diet and a low-salt diet decreased and increased WNK3 protein levels in mouse aortas, respectively. In contrast, KLHL2 was increased and decreased by a high-salt diet and a low-salt diet, respectively. As shown in Figure 2, C and D, the WNK3 protein level in the aortas of mice that were infused with AngII was increased and that of KLHL2 was decreased. These results indicate that salt intakes and AngII regulated WNK3 and KLHL2 protein levels in a reciprocal manner.

### AngII Rapidly Regulates KLHL2 and WNK3 Protein Levels and SPAK–NKCC1 Phosphorylation Cascade in MOVAS Cells

To investigate whether the regulation of WNK3 and KLHL2 by AngII that was observed in the aorta was, indeed, involved in the regulation of WNK3–SPAK–NKCC1 signaling, we performed cell culture studies using MOVAS cells. As shown in Figure 3, AngII rapidly decreased the KLHL2 protein levels in minutes, and WNK3, phosphorylated SPAK, and phosphorylated NKCC1 levels were also increased concomitantly. RT-PCR (Figure 4) revealed that both salt depletion in the mouse aorta and AngII

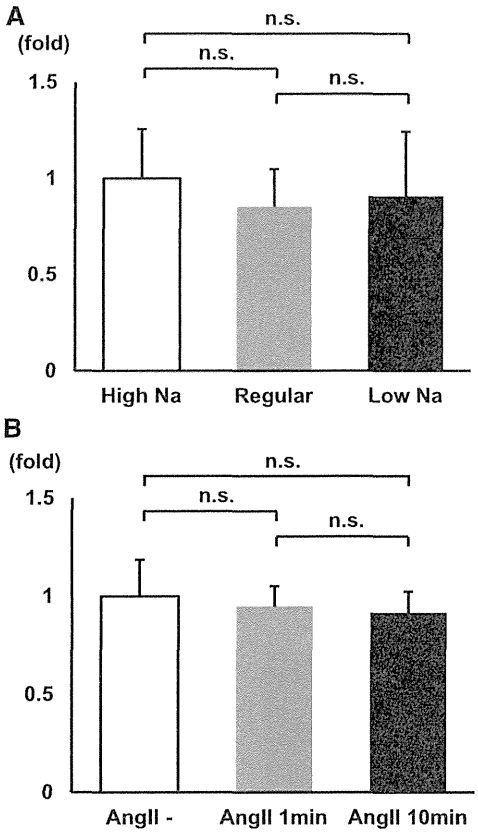


**Figure 4.** WNK3 mRNA levels in mouse aortas and MOVAS cells do not change with both salt intake and AngII. (A) WNK3 mRNA levels in mouse aortas under high-, regular-, and low-salt diets analyzed by quantitative RT-PCR. WNK3 mRNA levels in mouse aortas did not change with salt intake ($n$=11). (B) WNK3 mRNA levels of AngII-treated MOVAS cells were analyzed by quantitative RT-PCR. WNK3 mRNA levels in MOVAS did not increase with AngII treatment ($n$=3).

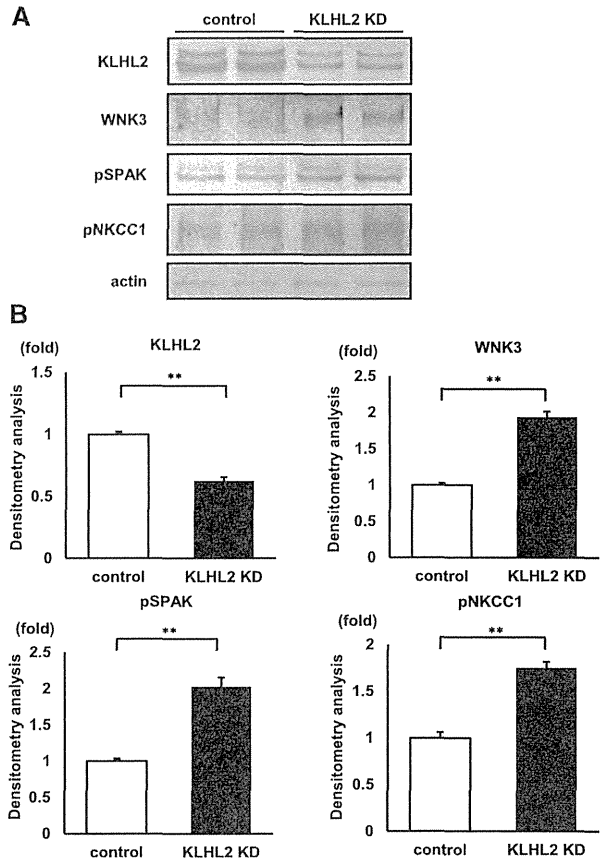


**Figure 5.** KLHL2 knockdown (KD) activates WNK3–SPAK–NKCC1 phosphorylation cascade in MOVAS cells. (A) Representative immunoblots and (B) densitometry analyses ($n$=14) of KLHL2, WNK3, phosphorylated SPAK (pSPAK), and phosphorylated NKCC1 (pNKCC1) in KLHL2 KD MOVAS cells. KLHL2 KD increased WNK3 expression and phosphorylation of SPAK and NKCC1. $^{**}P<0.01$.

treatment in MOVAS cells did not affect WNK3 mRNA levels, indicating that both regulatory increases in the WNK3 protein were not caused by the increased transcription of WNK3. Therefore, we then investigated the involvement of KLHL2 in the rapid regulation of WNK3 protein levels by AngII.

Although we have previously shown using WNK3 knockout mice that the AngII-induced activation of SPAK–NKCC1 signaling in the aorta was totally dependent on WNK3,[12] we also investigated the involvement of WNK1 and WNK4 in this regulation. However, WNK4 mRNA and protein were not detected in the mouse aorta and MOVAS cells (Supplemental Figure 2A). Therefore, whether WNK4 undergoes similar regulation by AngII remains to be determined. In contrast, the WNK1 protein was detected in the mouse aorta and MOVAS cells, and similar to WNK3, it was decreased by a high-salt diet and increased by a low-salt diet and AngII infusion (Supplemental Figure 2B). However, the AngII-induced phosphorylation of SPAK and NKCC1 was diminished in WNK3 knockdown MOVAS cells but not WNK1 knockdown cells (Supplemental Figure 3), confirming the dominant role of WNK3 in AngII-induced SPAK–NKCC1 signaling in the aorta and vascular smooth muscle cells.

### KLHL2 Regulates WNK3 Protein Levels in MOVAS Cells

To investigate whether the rapid regulation of WNK3 protein abundance was caused by KLHL2, we performed knockdown and overexpression experiments for KLHL2 in MOVAS cells. As shown in Figure 5, WNK3 was increased in KLHL2 knockdown cells, and the phosphorylation of SPAK and NKCC1 was also increased. However, KLHL2 overexpression decreased WNK3 protein levels and the phosphorylation of SPAK and NKCC1; however, Cul3 overexpression alone did not affect them. The inactivation of the WNK3–SPAK–NKCC1 cascade was more evident in both KLHL2- and Cul3-overexpressing cells (Figure 6), suggesting the importance of the complex formation of KLHL2–Cul3 as an E3 ligase in WNK3 regulation.[6] Thus, we performed a Cul3 knockdown experiment. As shown in Figure 7, Cul3 knockdown increased WNK3 protein under basal and AngII-stimulated conditions, showing the involvement of Cul3 in WNK3 degradation. Interestingly, KLHL2 protein was also increased by Cul3

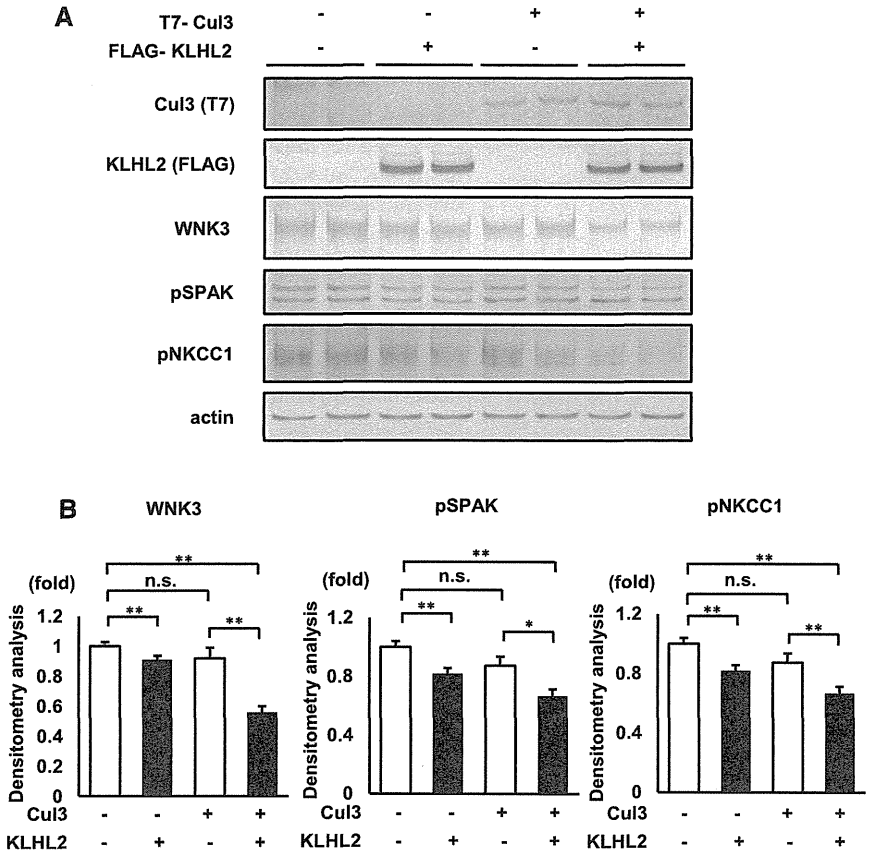


**Figure 6.** KLHL2 overexpression downregulates the WNK3–SPAK–NKCC1 phosphorylation cascade in MOVAS cells. (A) Representative immunoblots and (B) densitometry analyses ($n$=4) of KLHL2, WNK3, phosphorylated SPAK (pSPAK), and phosphorylated NKCC1 (pNKCC1) in Cul3- and KLHL2-overexpressing MOVAS cells. KLHL2 overexpression alone significantly decreased WNK3 expression and the phosphorylation of SPAK and NKCC1, and the coexpression of KLHL2 with Cul3 further downregulated the signal cascade; however, Cul3 overexpression alone did not affect the cascade. *$P$<0.05; **$P$<0.01.

knockdown, suggesting that KLHL2 protein may be regulated by Cul3-based E3 ligase as shown for KLHL3.[5] However, such an increase of KLHL2 did not lead to a reduction in WNK3 protein under the Cul3 knockdown condition, clearly suggesting that Cul3 is necessary for KLHL2-mediated WNK3 degradation. AngII could still decrease KLHL2 under the Cul3 knockdown condition (Figure 7), suggesting that the increased degradation of KLHL2 by AngII may be independent of Cul3.

Thus, AngII decreased KLHL2 protein by a Cul3-independent mechanism, and the decreased KLHL2–Cul3 E3 ligase increased WNK3 abundance, which activated the downstream SPAK–NKCC1 signaling.

### The Rapid Decrease in KLHL2 by AngII Is Caused by Autophagy-Mediated Degradation

Because KLHL2 was identified as the major regulator of WNK3 in MOVAS cells, we then investigated the mechanism of how the KLHL2 level was rapidly decreased by AngII. KLHL2 mRNA levels in MOVAS cells were not decreased with AngII treatment (Figure 8A). Furthermore, as shown in Figure 3, the decrease in KLHL2 induced by AngII was very rapid and occurred within minutes. Taken together, these data clearly indicate that the decrease in KLHL2 by AngII may be mediated by the activation of KLHL2 degradation.

To confirm this hypothesis and identify the degradation mechanism, we performed the experiments using protein degradation inhibitors. As shown in Figure 8, B and C and Supplemental Figure 4, chloroquine, an autophagy inhibitor, inhibited the decrease in KLHL2 by AngII treatment. In addition, other types of autophagy inhibitors (bafilomycin $A_1$ and 3-MA) showed similar effects. However, epoxomicin, a potent proteasome inhibitor, did not inhibit the decrease in KLHL2 by AngII (Figure 8, D and E). These results indicate that the KLHL2 decrease induced by AngII was caused by the activated degradation of KLHL2 through autophagy.

### Selective Autophagy Mediated by p62 Degrades KLHL2 on AngII Stimulation

Kelch-like ECH-associated protein 1 (Keap1), a member of the KLHL family (KLHL19), forms E3 ligase with Cul3 for NF E2-related factor 2, a novel regulator of the antioxidant response.[16] Recently, there have been some reports showing that Keap1 is degraded by selective autophagy mediated by sequestosome1/p62.[17,18] The experiments using protein degradation inhibitors strongly suggested that the KLHL2 degradation by AngII was not mediated by the proteasome system but by autophagy. Thus, we examined whether a mechanism similar to p62-mediated Keap1 degradation may be functioning on AngII-induced KLHL2 degradation by autophagy. We performed knockdown experiments of p62 in MOVAS cells. As shown in Figure 9, compared with the control cells, KLHL2 was increased in the p62 knockdown cells. Furthermore, p62 knockdown inhibited the decrease in KLHL2 by AngII stimulation. In another vascular smooth muscle cell line (rat vascular smooth muscle cells [SV40LT–SMC]), the same behavior was confirmed (Supplemental Figure 5). From these results, it was shown that the decrease in KLHL2 by AngII was mediated by selective autophagy facilitated by p62.

## DISCUSSION

In this study, we uncovered a new AngII signaling pathway in vascular smooth muscle cells for the control of vascular tone and BP. We had previously found that dietary salt intake and AngII regulate the WNK3–SPAK–NKCC1 phosphorylation

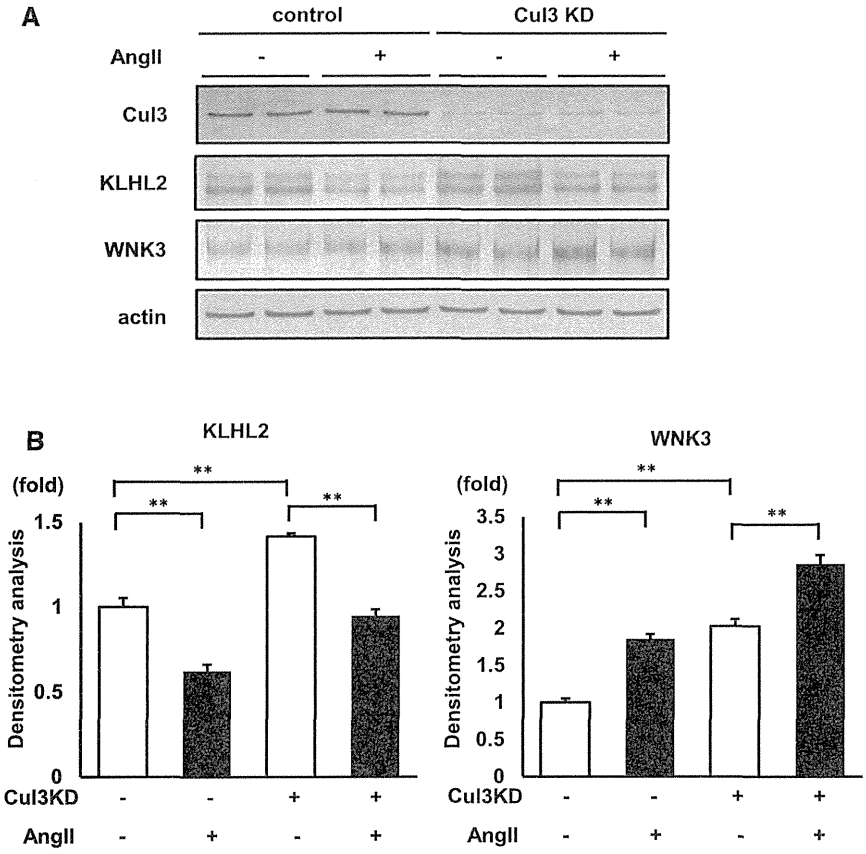


**Figure 7.** Cul3 knockdown (KD) increases WNK3 protein. (A) Representative immunoblots and (B) densitometry analyses ($n$=4) of Cul3, KLHL2, and WNK3 in Cul3 KD MOVAS cells. Cul3 KD increased WNK3 protein in both AngII(−) and AngII(+) conditions, suggesting the involvement of Cul3 in WNK3 degradation. AngII could still decrease KLHL2 in Cul3 KD MOVAS cells, suggesting a Cul3-independent degradation mechanism of KLHL2 by AngII. $^{**}P<0.01$.

cascade in MOVAS cells.[12] However, how AngII regulated this cascade remains unclear. We have now shown that AngII invoked p62-mediated selective autophagic degradation of KLHL2 acting as E3 ligase with Cul3 for WNK3 and that the reduction of KLHL2 led to the increase in WNK3 protein abundance, which activated the downstream phosphorylation signaling of SPAK–NKCC1 (Figure 10).

KLHL2 and KLHL3 are known to be involved in the degradation of WNK1/WNK2/WNK3/WNK4. Each of them forms a complex with Cul3 and acts as E3 ligase on WNK1/WNK2/WNK3/WNK4.[4–6,19,20] The KLHL3–Cul3 complex acts as an E3 ubiquitin ligase for WNK kinases, and KLHL3 mutations have been reported to cause PHAII through the impaired ubiquitination of WNK4.[4] However, the involvement of WNK kinase regulation by ubiquitination in the situation other than PHAII has not been identified. This may be the first report that a KLHL protein is, indeed, involved in the known physiologic regulation of the WNK signal cascade.

We showed that the AngII-induced WNK3 protein increase in MOVAS was surprisingly rapid, which was accompanied by the same rapid decrease in KLHL2. Knockdown and overexpression of KLHL2 were, indeed, able to regulate WNK3 protein abundance in MOVAS; this indicated that AngII-induced WNK3 signaling was mediated by the rapid regulatory decrease in the KLHL2 protein. In signal transduction, the regulation of key molecules by protein degradation may be a good mechanism that can promptly adapt to external stimuli, because there is no need for transcription and translation. The mechanism clarified in this study involves the regulation of degradation of two molecules (*i.e.*, KLHL2 and WNK3).

Autophagy is initially identified as a catabolic mechanism that protects against cellular starvation through the degradation of cellular components in lysosomes. In addition to such a classic role, autophagy has been shown to be involved in the regulation of numerous biologic processes, including signal transduction.[21] There have been some reports that showed the link between AngII and autophagy. Pan *et al.*[22] reported that AngII induced the downregulation of microRNA-30, which increased beclin-1 and induced excessive autophagy in cardiac myocytes. In the podocytes of the kidney, AngII elicited reactive oxygen species, which increased LC3-II and beclin-1 and induced autophagosomes.[23] Recently, in vascular smooth muscle cells, AngII also increased the autophagy levels through the activation of the AT1 receptor.[24] However, all of these reports showed that AngII could induce bulk autophagy but not selective autophagy mediated by p62; p62 is known as a key protein that can induce selective autophagy. In this study, it was first shown that KLHL2 was degraded by selective autophagy mediated by p62. In this respect, although additional information on how AngII regulated p62-mediated KLHL2 degradation remains to be determined, this report may describe the first selective autophagy mediated by AngII, which could be an important switching mechanism of signal transduction.

In this study, we clarified how AngII activated the WNK3–SPAK–NKCC1 phosphorylation cascade in MOVAS cells. This is the first demonstration that a KLHL protein physiologically regulates the WNK signal cascade and that AngII regulates its downstream signaling by autophagy. Thus, our study identified a novel component of signal transduction in AngII-induced vascular smooth muscle cell contraction, which could be a promising drug target for hypertension.

## CONCISE METHODS

### Dietary Salt and Drug Infusion Study Protocols

For experiments examining the effects of dietary salt intake, C57BL/6J mice were fed a high-salt diet (4% NaCl [wt/wt]), normal diet (0.9%

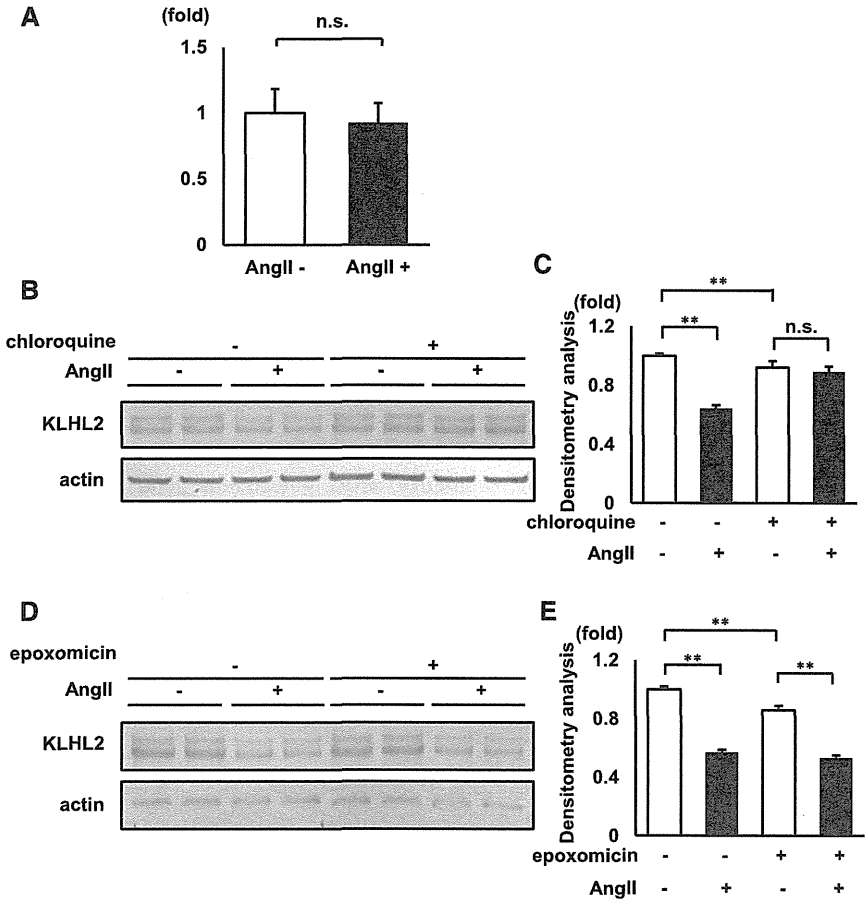


**Figure 8.** KLHL2 is degraded by the autophagy mechanism in MOVAS cells. (A) KLHL2 mRNA levels in AngII-treated MOVAS cells were analyzed by quantitative RT-PCR. KLHL2 mRNA in MOVAS cells did not decrease with AngII treatment ($n$=14). (B) Representative immunoblots and (C) densitometry analyses ($n$=6) of KLHL2 in MOVAS cells treated with chloroquine, a lysosomal degradation inhibitor. AngII did not decrease KLHL2 when MOVAS cells were treated with chloroquine. (D) Representative immunoblots and (E) densitometry analyses ($n$=6) of KLHL2 in MOVAS cells treated with epoxomicin, a proteasome inhibitor. AngII decreased KLHL2 in MOVAS cells treated with epoxomicin. $^{**}P<0.01$.

NaCl [wt/wt]), or low-salt diet (0.01% NaCl [wt/wt]) for 1 week. All foods were obtained from Oriental Yeast Co., Ltd.

For acute AngII infusion, we implanted the infusion tube into the right external jugular vein 5 days before the administration of AngII and infused AngII at a dose of 25 $\mu$g/g intravenously. The mice were then euthanized 30 minutes after AngII administration as reported previously.[8,12]

## Plasmids

Mouse KLHL2 cDNA was isolated by RT-PCR using mouse kidney mRNA from a C57BL/6J mouse. Sequences of the amplification primers used were as follows: KLHL2 sense, 5′-ATGGAGACGCCGCCACTGCCTCCCGC-3′; KLHL2 antisense, 5′-TCATAACGGTTTATCAATAACTGTGACC-3′. The mouse KLHL3 cDNA clone was purchased from Origene. Mouse KLHL2 and KLHL3 cDNA was cloned into 3XFLAG-CMV10 vector (Sigma-Aldrich).

## RT-PCR

Total RNA from the mouse aorta, mouse kidney, and MOVAS cells was extracted using TRIzol reagent (Invitrogen). The total RNA was reverse transcribed using Omniscript RT (Qiagen). Sequences of RT-PCR primers used were as follows: KLHL2 sense, 5′-TTCTTAACCTCGGCATC-3′; KLHL2 antisense, 5′-AACTCCTGTCTTACGTCCTT-3′; KLHL3 sense, 5′-GGACCAACACTTGGAAGCAG-3′; and KLHL3 antisense, 5′-AGTGCTCATGTTGGTGGG-3′. The WNK3 and WNK4 primers have been described previously.[12,25] The primers for GAPDH were purchased from TAKARA BIO.

## Cell Culture and Chemicals

We used the MOVAS cell line from mouse aorta (CRL-2797; ATCC) and the SV40LT-SMC Clone HEP-SA cell line from rat aorta (CRL-2018; ATCC) as a model of vascular smooth muscle cells. Both the MOVAS cells and SV40LT-SMC cells were cultured in DMEM supplemented with 10% (vol/vol) FBS, 2 mM L-glutamine, 100 units/ml penicillin, and 0.1 mg/ml streptomycin at 37°C in a humidified 5% $CO_2$ incubator. MOVAS cells that were cultured in six-well dishes were lysed with 150 $\mu$l ice-cold lysis buffer (50 mM Tris/HCl, pH 7.5, 150 mM NaCl, 1 mM EGTA, 1 mM EDTA, 50 mM sodium fluoride, 1 mM sodium orthovanadate, 1% Triton X-100, 0.27 M sucrose, 1 mM DTT, and Complete protease inhibitor cocktail; Roche; 1 tablet per 50 ml). In the p62 knockdown experiments, the cells were lysed with RIPA buffer containing 0.25 mM Tris/HCl (pH 8.0), 0.38% EGTA, 0.1 mM EDTA, 0.18% Na orthovanadate, 2.1% NaF, and Complete protease inhibitor cocktail (Roche; 1 tablet per 50 ml). After centrifugation at 12,000×$g$ for 5 minutes at 4°C, the supernatants were denatured for 20 minutes at 60°C with SDS sample buffer (Cosmo Bio) and subjected to SDS-PAGE.

For AngII stimulation experiments, the MOVAS cells were exposed to 5 $\mu$M AngII for 10 minutes. For the experiment using autophagy inhibitors, the cells were incubated with 25 $\mu$M chloroquine for 24 hours,[26] 200 nM bafilomycin $A_1$ for 24 hours,[27] or 5 mM 3-MA for 24 hours before AngII treatment.[26] As a proteasome inhibitor, we used 1 $\mu$M epoxomicin for 4 hours.[4]

## Transfection

The MOVAS cells were transfected by the indicated amount of plasmid DNA with Lipofectamine 2000 reagent (Invitrogen). For the KLHL2 knockdown experiments, we used 50 nM cocktails of three duplexes of siRNA for mouse KLHL2 (siTRIO Library; Origene) with Lipofectamine RNAiMAX (Invitrogen). The oligonucleotide sequences of siRNAs were as follows: mouse KLHL2 siTRIO SR417910A, agaauccugagaaacauugcccaCT; SR417910B, cgagcaaagagaguucgaauaaaGG; and SR417910C,

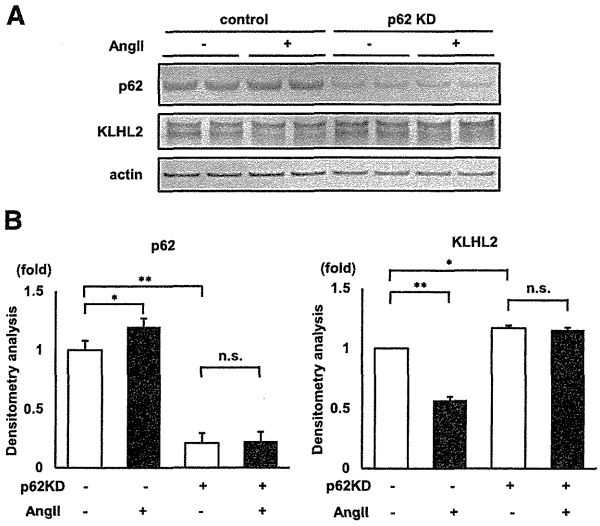


**Figure 9.** The decrease in KLHL2 by AngII is mediated by selective autophagy mediated by p62. (A) Representative immunoblots and (B) densitometry analyses ($n$=4) of p62 and KLHL2 in p62 knockdown (KD) MOVAS cells. p62 KD increased KLHL2 expression and inhibited the decrease in KLHL2 by AngII. $*P<0.01$; $**P<0.05$.

ccuuuaaagucaugaacgaacucAG. Experiments were performed at 48 hours after siRNA transfection. For the p62 knockdown experiments, we used 25 nM cocktails of three duplexes of siRNA for mouse p62 (siTRIO library; Origene) with Lipofectamine 2000 (Invitrogen). The oligonucleotide sequences of siRNAs were as follows: mouse p62 siTRIO SR413467A, ggcuccuacagaccaagaauuacGA; SR413467B, ggcuauguccuaugugaaagaugAC; and SR413467C, cgcaucuacauuaaagagaagaaGG. Experiments were performed at 24 hours after siRNA transfection. For the WNK1 or WNK3 knockdown experiments, we used 50 nM cocktails of three duplexes of siRNA for mouse WNK1 or WNK3 (siTRIO library; Origene) with Lipofectamine RNAiMAX (Invitrogen). The oligonucleotide sequences of siRNAs were as follows: mouse WNK1 siTRIO SR423399A, agaagaggcugaaauguuaaaggGT; SR423399B, gccagagccuaauggaauuaguaTT; and SR423399C, ccauucaaauaaaccaaacuugcTT and mouse WNK3 siTRIO SR423205A, gcagaaguucuaauaguuugacgGG; SR423205B, ggaccgcaaauuaacuaaagcugAG; and SR423205C, cgaauaucaagcauguauaccaaGT. Experiments were performed at 24 hours after siRNA transfection. For the Cul3 knockdown experiments, we used 100 nM cocktails of three duplexes of siRNA for mouse Cul3 (Santa Cruz Biotechnology) with Lipofectamine 2000 (Invitrogen). The oligonucleotide sequences of siRNAs were as follows: mouse Cul3 sc-35131A sense, ccaagcacaugaagacuauTT; sc-35131B sense, gaaggaauguuuagggauaTT; and sc-35131C sense, gacagaaaguagaugaugaTT. Experiments were performed at 36 hours after siRNA transfection. As a negative control, siTRIO negative control siRNA (Origene) was used.

## Immunoblotting

For the protein lysate of the mouse aorta, the thoracic aorta was carefully isolated and immediately frozen with liquid nitrogen. After being crushed with a mortar, the aorta was lysed with 150 $\mu$l lysis buffer, as reported previously, followed by centrifugation at 6000×$g$ at 4°C.[12,28] The supernatant (120 $\mu$l) was then denatured at 60°C for 20 minutes.

The primary antibodies used in this study were rabbit anti-KLHL2/KLHL3 antibody (Santa Cruz Biotechnology), anti-KLHL3 antibody (Proteintech), sheep anti-WNK3 antibody (S346C),[29,30] rabbit antiphosphorylated SPAK antibody,[31] rabbit antiphosphorylated NKCC1 (T206) antibody,[32] rabbit antiactin antibody (Cell Signaling Technology), anti-T7 antibody (EMD Millipore), anti-Cul3 antibody (BETHYL), anti-WNK1 antibody (A301–516A; BETHYL), anti-WNK4 antibody,[33] and rabbit anti-p62 antibody (Cell Signaling Technology). Alkaline phosphatase-conjugated anti-IgG antibodies (Promega) were used as secondary antibodies for immunoblotting. WesternBlue (Promega) was used for the development of immunoblots. The relative intensities of the immunoblot bands were determined by densitometry with ImageJ software.

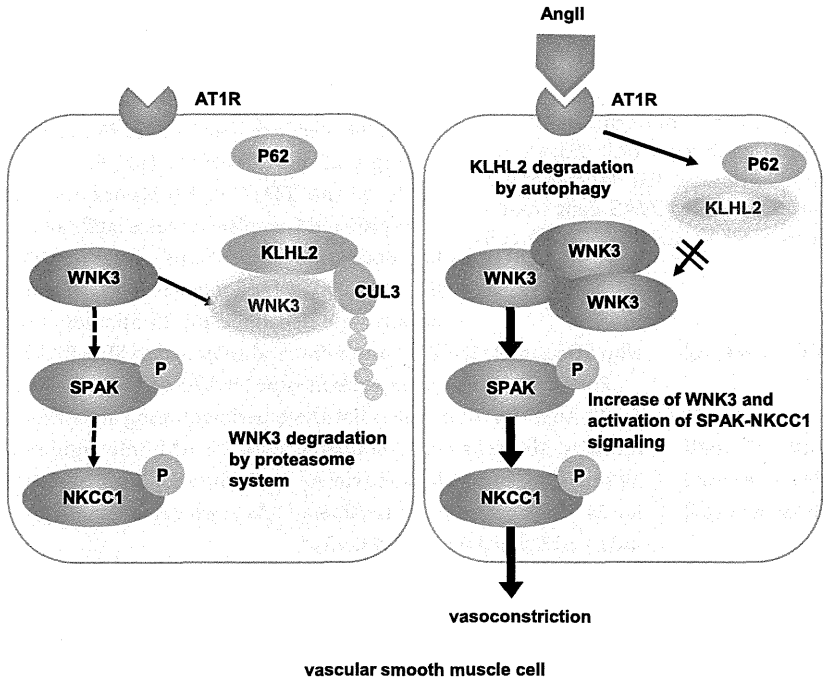


**Figure 10.** The mechanism of vasoconstriction mediated AngII–KLHL2–WNK3 signaling. In vascular smooth muscle cells, WNK3 is degraded by KLHL2–CUL3-mediated ubiquitination. With AngII stimulation, KLHL2 is degraded by selective autophagy by p62, which leads to the activation of the WNK3–SPAK–NKCC1 phosphorylation cascade and vasoconstriction. AT1R, angiotensin II type-I receptor; P, phosphorylation.

## Statistical Analyses

Statistical significance was evaluated using an unpaired $t$ test. All data were expressed as means±SEMs. When more than three groups were compared, one-way ANOVA with Fischer's *post hoc* test was used. $P$ values<0.05 were considered to indicate statistical significance.

## ACKNOWLEDGMENTS

We thank M. Chiga and C. Iijima for help in the experiments. We also thank D. Alessi for provision of antibodies.

This study was supported, in part, by Japan Society for the Promotion of Science Grants-in-Aid for Scientific Research (S, A); a Ministry of Education, Culture, Sports, Science and Technology of Japan Grant-in-Aid for Young Scientists (B); a Ministry of Health, Labor, and Welfare Health and Labor Sciences Research Grant; Salt Science Research Foundation Grant 1422; the Takeda Science Foundation; a Banyu Foundation Research Grant; and the Vehicle Racing Commemorative Foundation.

## DISCLOSURES

None.

## REFERENCES

1. Boyden LM, Choi M, Choate KA, Nelson-Williams CJ, Farhi A, Toka HR, Tikhonova IR, Bjornson R, Mane SM, Colussi G, Lebel M, Gordon RD, Semmekrot BA, Poujol A, Välimäki MJ, De Ferrari ME, Sanjad SA, Gutkin M, Karet FE, Tucci JR, Stockigt JR, Keppler-Noreuil KM, Porter CC, Anand SK, Whiteford ML, Davis ID, Dewar SB, Bettinelli A, Fadrowski JJ, Belsha CW, Hunley TE, Nelson RD, Trachtman H, Cole TR, Pinsk M, Bockenhauer D, Shenoy M, Vaidyanathan P, Foreman JW, Rasoulpour M, Thameem F, Al-Shahrouri HZ, Radhakrishnan J, Gharavi AG, Goilav B, Lifton RP: Mutations in kelch-like 3 and cullin 3 cause hypertension and electrolyte abnormalities. *Nature* 482: 98–102, 2012
2. Wilson FH, Disse-Nicodème S, Choate KA, Ishikawa K, Nelson-Williams C, Desitter I, Gunel M, Milford DV, Lipkin GW, Achard JM, Feely MP, Dussol B, Berland Y, Unwin RJ, Mayan H, Simon DB, Farfel Z, Jeunemaitre X, Lifton RP: Human hypertension caused by mutations in WNK kinases. *Science* 293: 1107–1112, 2001
3. Louis-Dit-Picard H, Barc J, Trujillano D, Miserey-Lenkei S, Bouatia-Naji N, Pylypenko O, Beaurain G, Bonnefond A, Sand O, Simian C, Vidal-Petiot E, Soukaseum C, Mandet C, Broux F, Chabre O, Delahousse M, Esnault V, Fiquet B, Houillier P, Bagnis CI, Koenig J, Konrad M, Landais P, Mourani C, Niaudet P, Probst V, Thauvin C, Unwin RJ, Soroka SD, Ehret G, Ossowski S, Caulfield M; International Consortium for Blood Pressure (ICBP)Bruneval P, Estivill X, Froguel P, Hadchouel J, Schott JJ, Jeunemaitre X: KLHL3 mutations cause familial hyperkalemic hypertension by impairing ion transport in the distal nephron. *Nat Genet* 44: 456–460, 2012
4. Wakabayashi M, Mori T, Isobe K, Sohara E, Susa K, Araki Y, Chiga M, Kikuchi E, Nomura N, Mori Y, Matsuo H, Murata T, Nomura S, Asano T, Kawaguchi H, Nonoyama S, Rai T, Sasaki S, Uchida S: Impaired KLHL3-mediated ubiquitination of WNK4 causes human hypertension. *Cell Rep* 3: 858–868, 2013
5. Ohta A, Schumacher FR, Mehellou Y, Johnson C, Knebel A, Macartney TJ, Wood NT, Alessi DR, Kurz T: The CUL3-KLHL3 E3 ligase complex mutated in Gordon's hypertension syndrome interacts with and ubiquitylates WNK isoforms: Disease-causing mutations in KLHL3 and WNK4 disrupt interaction. *Biochem J* 451: 111–122, 2013
6. Takahashi D, Mori T, Wakabayashi M, Mori Y, Susa K, Zeniya M, Sohara E, Rai T, Sasaki S, Uchida S: KLHL2 interacts with and ubiquitinates WNK kinases. *Biochem Biophys Res Commun* 437: 457–462, 2013
7. Chiga M, Rai T, Yang SS, Ohta A, Takizawa T, Sasaki S, Uchida S: Dietary salt regulates the phosphorylation of OSR1/SPAK kinases and the sodium chloride cotransporter through aldosterone. *Kidney Int* 74: 1403–1409, 2008
8. Talati G, Ohta A, Rai T, Sohara E, Naito S, Vandewalle A, Sasaki S, Uchida S: Effect of angiotensin II on the WNK-OSR1/SPAK-NCC phosphorylation cascade in cultured mpkDCT cells and in vivo mouse kidney. *Biochem Biophys Res Commun* 393: 844–848, 2010
9. Takahashi D, Mori T, Nomura N, Khan MZ, Araki Y, Zeniya M, Sohara E, Rai T, Sasaki S, Uchida S: WNK4 is the major WNK positively regulating NCC in the mouse kidney. *Biosci Rep* 34: e00107, 2014
10. Nishida H, Sohara E, Nomura N, Chiga M, Alessi DR, Rai T, Sasaki S, Uchida S: Phosphatidylinositol 3-kinase/Akt signaling pathway activates the WNK-OSR1/SPAK-NCC phosphorylation cascade in hyperinsulinemic db/db mice. *Hypertension* 60: 981–990, 2012
11. Saritas T, Borschewski A, McCormick JA, Paliege A, Dathe C, Uchida S, Terker A, Himmerkus N, Bleich M, Demaretz S, Laghmani K, Delpire E, Ellison DH, Bachmann S, Mutig K: SPAK differentially mediates vasopressin effects on sodium cotransporters. *J Am Soc Nephrol* 24: 407–418, 2013
12. Zeniya M, Sohara E, Kita S, Iwamoto T, Susa K, Mori T, Oi K, Chiga M, Takahashi D, Yang SS, Lin SH, Rai T, Sasaki S, Uchida S: Dietary salt intake regulates WNK3-SPAK-NKCC1 phosphorylation cascade in mouse aorta through angiotensin II. *Hypertension* 62: 872–878, 2013
13. Orlov SN, Koltsova SV, Tremblay J, Baskakov MB, Hamet P: NKCC1 and hypertension: Role in the regulation of vascular smooth muscle contractions and myogenic tone. *Ann Med* 44[Suppl 1]: S111–S118, 2012
14. Dowd BF, Forbush B: PASK (proline-alanine-rich STE20-related kinase), a regulatory kinase of the Na-K-Cl cotransporter (NKCC1). *J Biol Chem* 278: 27347–27353, 2003
15. Ponce-Coria J, San-Cristobal P, Kahle KT, Vazquez N, Pacheco-Alvarez D, de Los Heros P, Juárez P, Muñoz E, Michel G, Bobadilla NA, Gimenez I, Lifton RP, Hebert SC, Gamba G: Regulation of NKCC2 by a chloride-sensing mechanism involving the WNK3 and SPAK kinases. *Proc Natl Acad Sci U S A* 105: 8458–8463, 2008
16. Itoh K, Wakabayashi N, Katoh Y, Ishii T, Igarashi K, Engel JD, Yamamoto M: Keap1 represses nuclear activation of antioxidant responsive elements by Nrf2 through binding to the amino-terminal Neh2 domain. *Genes Dev* 13: 76–86, 1999
17. Komatsu M, Kurokawa H, Waguri S, Taguchi K, Kobayashi A, Ichimura Y, Sou YS, Ueno I, Sakamoto A, Tong KI, Kim M, Nishito Y, Iemura S, Natsume T, Ueno T, Kominami E, Motohashi H, Tanaka K, Yamamoto M: The selective autophagy substrate p62 activates the stress responsive transcription factor Nrf2 through inactivation of Keap1. *Nat Cell Biol* 12: 213–223, 2010
18. Fan W, Tang Z, Chen D, Moughon D, Ding X, Chen S, Zhu M, Zhong Q: Keap1 facilitates p62-mediated ubiquitin aggregate clearance via autophagy. *Autophagy* 6: 614–621, 2010
19. Shibata S, Zhang J, Puthumana J, Stone KL, Lifton RP: Kelch-like 3 and Cullin 3 regulate electrolyte homeostasis via ubiquitination and degradation of WNK4. *Proc Natl Acad Sci U S A* 110: 7838–7843, 2013
20. Wu G, Peng JB: Disease-causing mutations in KLHL3 impair its effect on WNK4 degradation. *FEBS Lett* 587: 1717–1722, 2013
21. Boya P, Reggiori F, Codogno P: Emerging regulation and functions of autophagy. *Nat Cell Biol* 15: 713–720, 2013
22. Pan W, Zhong Y, Cheng C, Liu B, Wang L, Li A, Xiong L, Liu S: MiR-30-regulated autophagy mediates angiotensin II-induced myocardial hypertrophy. *PLoS ONE* 8: e53950, 2013
23. Yadav A, Vallabu S, Arora S, Tandon P, Slahan D, Teichberg S, Singhal PC: ANG II promotes autophagy in podocytes. *Am J Physiol Cell Physiol* 299: C488–C496, 2010
24. Yu KY, Wang YP, Wang LH, Jian Y, Zhao XD, Chen JW, Murao K, Zhu W, Dong L, Wang GQ, Zhang GX: Mitochondrial KATP channel involvement in angiotensin II-induced autophagy in vascular smooth muscle cells. *Basic Res Cardiol* 109: 416, 2014
25. O'Reilly M, Marshall E, Macgillivray T, Mittal M, Xue W, Kenyon CJ, Brown RW: Dietary electrolyte-driven responses in the renal WNK kinase pathway in vivo. *J Am Soc Nephrol* 17: 2402–2413, 2006
26. Bae SH, Sung SH, Oh SY, Lim JM, Lee SK, Park YN, Lee HE, Kang D, Rhee SG: Sestrins activate Nrf2 by promoting p62-dependent